Geologia Croatica
Journal of the Croatian Geological Survey and the Croatian Geological Society
2026 | 79/3 | 271–289 | 6 Figs. | 1 Tab. | 1 Suppl. | www.geologia-croatica.hr

A ≈ 3.0 Ga zircon core in an Early Cambrian (meta)granitoid from the basement of Mt Papuk (Croatia): a trifle or treasure for palaeogeographic reconstructions?

Dražen Balen[1], Etienne Skrzypek[2], Daniela Gallhofer[2], Petra Schneider[1,*] and Christoph A. Hauzenberger[2]

[1,*] University of Zagreb, Faculty of Science, Department of Geology, Horvatovac 102a, 10000 Zagreb, Croatia; (drbalen@geol.pmf.unizg.hr, corresponding author: pschneider@geol.pmf.unizg.hr)
[2] University of Graz, Department of Earth Sciences, NAWI Graz Geocenter, Universitätsplatz 2, 8010 Graz, Austria; (etienne.skrzypek@uni-graz.at, daniela.gallhofer@uni-graz.at, christoph.hauzenberger@uni-graz.at)

doi: 10.4154/gc.2026.14

CC BY
Crossref Similarity Check

Original scientific paper

Article history:
Manuscript received: April 14, 2026
Revised manuscript accepted: July 21, 2026
Available online: October 8, 2026

Abstract

The U-Pb age spectrum of zircon grains including rim and xenocrystic core domains from an Early Cambrian peraluminous (meta)granitoid in the eastern part of Mt. Papuk (Croatia) was determined using laser ablation inductively coupled plasma mass spectrometry. Zircon cathodoluminescence images reveal an unusually high proportion of xenocrystic cores surrounded by oscillatory-zoned magmatic rims. The U-Pb age spectrum displays a prominent cluster at ca. 535 Ma (Ediacaran–Cambrian), interpreted as the crystallisation age, and a skewed one towards ca. 498 Ma (Cambrian–Ordovician), interpreted as a Cenerian thermal event superimposed on the Cadomian granitoid crystallisation age. Xenocrystic zircon cores yield several age groups and single ages within a Pan-African cluster at ≈ 0.65–0.8 Ga, along with clusters from detrital sources between 0.8 and 3.0 Ga. The age spectrum, analysed by the frequency ratio of Proterozoic to Archean zircon ages, the shape of a kernel density estimate curve, and a multidimensional scaling plot, indicates a provenance of zircon grains that is typical for the western part of northern Gondwana, particularly the Saharan Metacraton, with contributions from the Arabian–Nubian shield and the West African craton, where transport to the distant northern Gondwana margin occurred from their hinterland. The granitoid crystallisation age of 535.3 ± 0.9 I 7.1 Ma (age ± 2SE uncertainty I total 2SE including systematic uncertainties) represents the "oldest dated rock" in Croatia, while among the xenocrystic zircon cores, the oldest zircon in Croatia measured so far has a $^{207}Pb/^{206}Pb$ date of 3061±27 Ma (Mesoarchean).

Keywords: Mesoarchean zircon, Saharan Metacraton, Cambrian peraluminous (meta) granitoid, Cenerian orogeny, Cadomian orogeny

1. INTRODUCTION

Given the usually relatively small proportion of ancient (>3 Ga) dates recorded in zircons from basement precursors in the Carpathians and Alps (e.g., ŽÁK et al., 2021; CHANG et al., 2021; SIEGESMUND et al., 2018, 2021), either as inherited cores or single grains, one may wonder about the geological significance of reporting such scarce data, which are often unrelated to the surrounding geological record. What is intended beyond the catchy phrase "the oldest" mineral, rock or fossil, etc., for a particular area? Is the purpose of such a record merely to temporarily document "the oldest" feature, a record that in its "glory" will undoubtedly not last long? Or is it possible to extract scientific or practical value from a single, often isolated point in the timescale? Could the collection of such scarce data serve to reconstruct the early evolution of the continental crust and the geodynamic processes that formed ancient orogens?

The area of Croatia, with the Dinarides and Pannonian Basin as its main geological features, has been a highly dynamic area, and is currently characterised by active tectonics, earthquakes or erosion (e.g., CROATIAN GEOLOGICAL SURVEY, 2009). The geodynamic processes, occurring over vast temporal and spatial scales and represented by different orogenic cycles, do not favour the preservation of ancient geological material and, consequently, the preservation of their ages. However, a substantial number of Variscan dates were recorded in spite of the Alpine evolution of the Dinarides and the Pannonian Basin, as well as the Variscan evolution of their basements, which limits but does not prevent opportunities to find records of pre-Variscan events inside basement crystalline rocks. Among these, the most promising areas are the Mt. Papuk and Mt. Psunj regions of the Slavonian Mts., where, in the last 20 years, Alpine (e.g., BIŠEVAC et al., 2010; BALEN et al., 2013, 2018a; SCHNEIDER et al., 2022, 2025), Variscan (HORVÁTH et al., 2010; HORVAT et al., 2018; SKRZYPEK et al., 2025), and pre-Variscan (BALEN et al., 2006, 2015; HORVÁTH et al., 2010; SLOVENEC et al., 2020; STARIJAŠ MAYER et al., 2023; GALLHOFER et al., 2026) igneous and metamorphic events have been documented.

With recent analytical advances, particularly of *in situ* isotopic techniques on single mineral grains, zircon age spectra have become a powerful tool for understanding evolutionary

processes far beyond the age of formation of the host rock. The aim of this report is to present the age spectrum of zircon grains from a (meta)granitoid that contains abundant xenocrystic zircon cores related to the Cadomian and/or Cenerian orogenies, but also to the interior of Gondwana cratons. We compare xenocrystic core ages with detrital zircon age spectra of the main Gondwana sources, discuss potential source terrains and highlight their potential for palaeogeographic interpretations. Furthermore, we provide petrographic and geochemical descriptions of the (meta)granitoid sample, along with full documentation of the U-Pb zircon dating results. We report the discovery of a ≈ 3.0 Ga old zircon core, which is currently the oldest mineral in Croatia and an Early Palaeozoic / Ediacaran magmatic crystallisation age for the (meta)granitoid, which, to our current knowledge, represents the oldest robustly dated rock in Croatia.

2. GEOLOGICAL BACKGROUND

The Slavonian Mts. comprise several *inselbergs* of crystalline basement that emerge from the sedimentary infill of the southwestern Pannonian Basin (Fig. 1a). Among them, Mt. Papuk exposes a significant area of pre-Variscan and Variscan igneous and metamorphic rocks. On a large scale, Mt. Papuk is part of the Tisia (Tisza, Tisa, Tisija) Mega-Unit, a continental fragment of Europe, separated in the Middle Jurassic during opening of the eastern branch of the Alpine Tethys Ocean (e.g., PAMIĆ et al., 2002; SCHMID et al., 2008). The pre-Alpine crystalline basement rocks at Mt. Papuk are traditionally divided into three complexes (JAMIČIĆ, 1983, 1988), defined on the basis of field observations, petrography and structural geology: (1) the Psunj metamorphic complex (also called the Kutjevo metamorphic series), a low- to medium-grade metamorphic complex composed of chlorite-schist, phyllite, micaschist, paragneiss, amphibolite and marble, with additional small bodies of granite; (2) the Papuk metamorphic complex (also called the Jankovac metamorphic series) composed of S-type granites intruding medium- to high-grade rocks including amphibolite, micaschist and locally migmatitic gneiss; and (3) the tectonically uppermost Radlovac complex, consisting of very low- to low-grade slate, meta-greywacke, meta-conglomerate and phyllite, locally intruded by metabasic rocks. Such geological evolution is interpreted as comprising three phases of sedimentation and metamorphism in periods from the Precambrian(?) to the Upper Permian.

An early Palaeozoic or late Neoproterozoic and a pre-Variscan metamorphic event were suggested for some rocks (JAMIČIĆ, 1983, 1988; JAMIČIĆ & BRKIĆ, 1987), but without geochronological evidence or stratigraphic support: (1) the Psunj metamorphic complex is assumed to have formed by metamorphism during the Baikalian orogeny (in the Late Precambrian, i.e. ≈ 850–650 Ma), which affected the supposed Precambrian psammitic and pelitic sediments and submarine volcanic rocks, and was later overprinted and retrogressed by younger metamorphic events; (2) the Papuk metamorphic complex underwent metamorphism and migmatitisation during the Caledonian orogeny (Ordovician to Early Devonian, i.e. ≈ 490–390 Ma), which affected the inferred Lower Palaeozoic pelitic sediments and volcanic rocks; and (3) the Radlovac metamorphic complex was subject to very low-grade metamorphism during the Variscan orogeny (Late Palaeozoic, i.e. ≈ 380–280 Ma), affecting the clastic sediments of Upper Devonian, Carboniferous and up to Middle Permian depositional ages.

Based on K-Ar and Rb-Sr dating, PAMIĆ et al. (1988) and PAMIĆ & LANPHERE (1991) combined the first two complexes into the "Progressively Metamorphosed Complex" (PMC). The PMC is considered to have formed predominantly during Variscan tectono-metamorphic event(s) (PAMIĆ & LANPHERE, 1991). In the Late Cretaceous, the PMC was intruded by postmetamorphic dyke swarms of basalt, andesite and rhyolite (e.g., SCHNEIDER et al., 2022, 2025).

More detailed data for pre-Variscan events include the following ages and P-T estimates: electron microprobe (EMPA) ages obtained on monazite of 444 ± 19 Ma and 428 ± 25 Ma for amphibolite facies micaschist (BALEN et al., 2006); monazite ages of 528 ± 7 Ma and 465 ± 7 Ma (from reaction textures), 616 ± 23 Ma (monazite inclusions in garnet cores), 491 ± 6 Ma (monazite inclusions in garnet rims) and 417 ± 20 Ma (monazite in matrix) for an amphibolite facies orthogneiss (BALEN et al., 2015); a Lu-Hf garnet–whole-rock isochron age of 466.0 ± 2.3 Ma for a chlorite–muscovite–garnet schist and a monazite age of 471 ± 15 Ma for amphibolite facies metapelites (STARIJAŠ MAYER et al., 2023); a ^{40}Ar-^{39}Ar amphibole age of 487.1 ± 4.3 Ma and a Sm-Nd isochron age of 503 ± 13 Ma for a gabbroic rock (SLOVENEC et al., 2020). Although even older ages and events have been reported for the Slavonian Mts., they either lack adequate analytical support (JAMIČIĆ, 1983), or use analytical methods such as K-Ar (including whole rock), that cannot distinguish between polycyclic events (PAMIĆ et al., 1988; PAMIĆ & LANPHERE 1991). This brief overview shows that, even when single dates are included, no robust ages older than the Cambrian or Ediacaran have been found.

3. METHODS

A sample of (meta)granitoid (KU1A; ≈ 20×20×10 cm in size, yielding ≈ 10 kg of material) was crushed to separate zircon grains using a standard extraction procedure involving sieving, panning, and magnetic separation with a hand magnet and a Frantz isodynamic magnetic separator. For further analysis, randomly hand-picked zircon grains were mounted in epoxy resin, grounded to expose their interiors and polished with diamond paste. To observe internal zoning patterns and xenocrystic cores, the grain mounts were imaged with a ZEISS DSM 982 (Gemini) field emission scanning electron microscope (SEM) at the Department of Earth Sciences (NAWI Graz Geocenter, University of Graz). In the cathodoluminescence (CL) images, zircon grains with inherited cores were common and easily identified. The presence and size of internal domains influenced the selection of ablation spot sites.

The first session of isotopic analyses of zircon (03/09/2025) was conducted at the Department of Earth Sciences (NAWI Graz Geocentre, University of Graz). An ESI NWR 193 nm ArF Excimer Laser was used to ablate material for 30 s with a 35 μm spot diameter, 10 Hz frequency, and a fluence of approximately 4.5 J/cm². The ablated material was transported to an Agilent 7900 series single-collector quadrupole ICP-MS

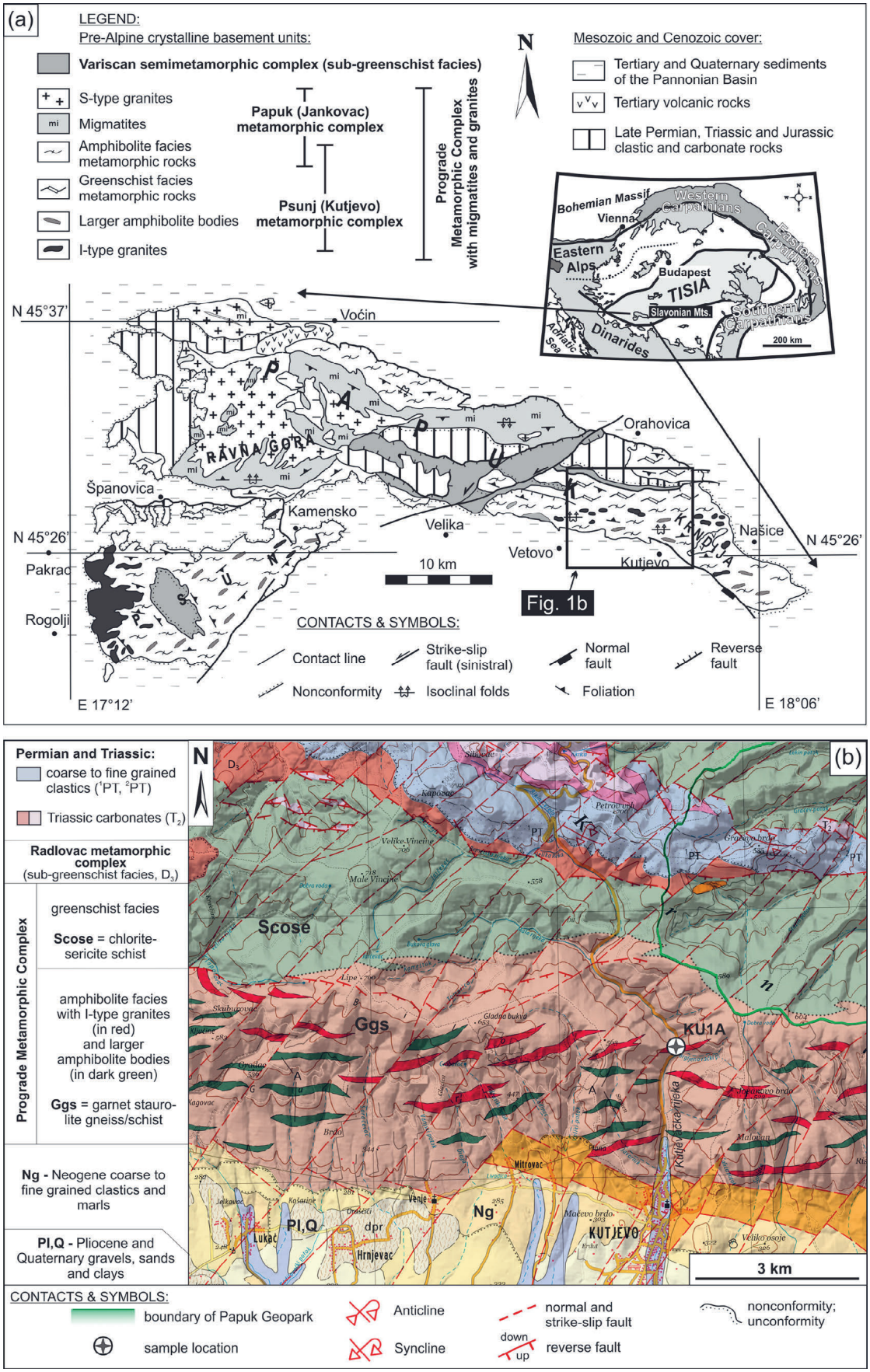

Figure 1. (**a**) A simplified geological map of the Slavonian Mts. (geological base map after JAMIČIĆ (1988) and PAMIĆ & LANPHERE (1991)). More details of the Mt. Papuk area can be found on the Basic Geological Map of SFRY 1:100 000 sheets and explanatory notes for Daruvar and Orahovica by JAMIČIĆ (1989), JAMIČIĆ & BRKIĆ (1987) and JAMIČIĆ et al. (1987, 1989). The index map shows the position of the Slavonian Mts. relative to major mountain chains and the Tisia Mega-Unit; (**b**) A detailed geological and topographic map of the study area (modified geological map after JAMIČIĆ, 1983, 1988; JAMIČIĆ & BRKIĆ, 1987; JAMIČIĆ et al., 1987) showing the location of the outcrop (KU1A).

system where ^{202}Hg, ^{204}(Hg+Pb), ^{206}Pb, ^{207}Pb, ^{208}Pb, ^{232}Th and ^{238}U were monitored.

The second session of zircon age dating (28/11/2025) was performed at the Central Lab for Water, Minerals and Rocks, NAWI Graz Geocentre, Graz University of Technology and University of Graz, using a Nu Plasma II high-resolution multi-collector ICP-MS (Nu Instruments), coupled with an ESI NWR 193 nm ArF Excimer Laser. Analytical conditions for age dating included 15 s of sample ablation with a spot diameter of 15 μm, a repetition rate of 5 Hz and a laser fluence of approximately 2.4 J/cm². The same masses as in the first session were monitored.

Reference zircons 91500 (WIEDENBECK et al., 1995) (Agilent 7900) and GJ1 (JACKSON et al., 2004) (Nu Plasma II) were used as primary calibration materials. The following zircons were used for quality control: M257 (NASDALA et al., 2008), 91500 (WIEDENBECK et al., 1995), Plešovice (SLÁMA et al., 2008), KARA-18 (IAG reference zircon, G-Chron round 2) and NIST SRM 610 glass (JOCHUM et al., 2011) to verify the reproducibility and accuracy of the analyses. In the first session of dating, the measurement sequences consisted of: one spot on NIST SRM 610 glass, followed by three spots on zircon 91500, one spot on Plešovice and M257 zircon and 15 spots on sample KU1A. In the second session of dating, the measurement sequences consisted of: one spot on NIST SRM 610 glass, followed by three spots on zircon GJ1, one spot on zircon M257, 91500 and KARA, and 12 spots on sample KU1A. Further details can be found in Supplementary Table 1.

Data were reduced using the IOLITE v. 3.71 software package with the X_U-Pb_Geochron4 DRS (PATON et al., 2010, 2011). IsoplotR software (VERMEESCH, 2018) was used for plotting and age calculations. No common lead correction was applied. The accuracy of the secondary reference zircons Plešovice, 91500, M257 and Kara-18 is reported as the relative offset from the TIMS ^{206}Pb/^{238}U age and was better than 2 % in both measurement sessions. The ^{206}Pb/^{238}U weighted mean ages of the samples were calculated from single zircon dates with 90−110 % concordance (concordance = (^{206}Pb/^{238}U date) / (^{207}Pb/^{235}U date) × 100). Systematic uncertainties, including the long-term excess variance of ^{206}Pb/^{238}U for the validation zircons (≈ 1.3 %), were propagated by quadratic addition to the uncertainty of the ^{206}Pb/^{238}U weighted mean ages, following the recommendations of HORSTWOOD et al. (2016).

4. RESULTS

4.1. Field observations

The study focuses on zircon grains from a (meta)granitoid sample collected in the eastern part of Mt. Papuk (Croatia, Tisia Mega-Unit, Pannonian Basin basement). There, small igneous bodies (up to several tens of metres wide) of "I-type" granitoids after PAMIĆ & LANPHERE (1991) are associated with pre-Variscan metamorphic rocks. Amphibolite, paragneiss, and micaschist from the same outcrop (N 45°26'57'', E 17°53'15'') have been investigated by BALEN et al. (2006) and HORVÁTH et al. (2010) as part of a transect of medium-grade metamorphic rocks (Fig. 1b) along the Kutjevačka rijeka (Kutjevo River). The outcrop, a designated geosite of the UNESCO Global Geopark Papuk (geosite 1), displays centimetre- to decimetre-scale alternating layers of strongly foliated amphibolite-facies metamorphic rocks (amphibolite, paragneiss and micaschist), that occasionally preserve relicts of microscale isoclinal folds and mylonitic microstructures. The (meta)granitoid is enclosed within metamorphic rocks and occurs as a small, tens to hundreds of metres sized, cataclastised plutonic body concordant with the foliation. In this study, two (meta)granitoids from the same igneous body near Kutjevo were compared: the first was based on previous reports (BALEN et al., 2018b, c), and the second (KU1A) is the sample analysed here.

4.2. Petrography and geochemistry of the Kutjevo (meta)granitoid

The studied rock is dark grey, medium-grained (up to ≈ 0.3 cm), and has an almost granite-like appearance with biotite-rich layers (Fig. 2a). The largely preserved isotropic (granitoid) structure consists of subhedral to rounded, 2–3 mm sericitised plagioclase with typical twinning (andesine $An_{32–46}$ and rare albite grains), quartz, zoned garnet rich in the almandine component (Sps_{02-05}, Prp_{05-17}, Alm_{66-74}, $Grs+And_{07-23}$), amphibole, partially chloritized biotite and K-feldspar (Fig. 2b–d). Accessory minerals include ilmenite, titanite, clinozoisite, zircon and apatite (Fig. 2e).

The (meta)granitoid sample (KU1A) is a peraluminous (A/NK = 2.19–2.23, A/CNK = 1.02–1.14) diorite to monzonite, with SiO_2=56.12–57.55 wt%, $Na_2O + K_2O$ = 5.99–6.09 wt% and $Fe_2O_3 + MgO$ = 8.15–8.24 wt%, containing only 80 μg/g of rare earth elements (REE). It has lower Th (1.7 μg/g), Nb (4.2 μg/g), Ce (26.4 μg/g) and Ti (0.99–1.02 wt% TiO_2) values and higher U (0.7 μg/g), Pb (9.6 μg/g), Sr (485–664 μg/g), Zr (203–271 μg/g) and Eu (1.34 μg/g) values than the primitive mantle, while a slight enrichment in the light REE (LREE; La_N/Sm_N = 2.22, Gd_N/Lu_N = 1.55) and Eu/Eu* = 1.03 relative to chondrite are observed. The zircon saturation temperature (740–800 °C, calibration after BOEHNKE et al., 2013; bearing in mind that the calculated temperature may be influenced by inherited zircons) indicates that zircon crystallised at a relatively high temperature (BALEN et al., 2018b), while the abundance of garnet and the absence of cordierite indicate pressures between 600 and 900 MPa.

4.3. Zircon characteristics and age spectrum

Zircon grains are characterised by {100} > {110} prisms and {101} < {211} bipyramids. The zircon grains are mainly clear, prismatic or stubby with lengths of approximately 100 μm and widths of about 40–60 μm, giving aspect ratios close to ≈ 2:1 (Fig. 2f). They generally preserve their euhedral shape and are not broken. A range of crystallographic shapes and typologies is observed, with a dominance of S_7, S_{12} and L_2 types (after PUPIN, 1980).

High mean U (455 μg/g) and Th (138 μg/g) contents, a Zr/Hf ratio of 30.3 and a Ti-in-zircon temperature of 760 °C (calibration after WATSON et al., 2006) together with the REE patterns of zircon normalised to chondrite that show a positive Ce anomaly (Ce/Ce* = 16.6) and a negative Eu

anomaly (Eu/Eu* = 0.44) (BALEN et al., 2018b), are typical for continental crust and zircon crystallised from a felsic magmatic source (e.g., BELOUSOVA et al., 2002). The $^{206}Pb/^{238}U$ date obtained previously on zircon is 554±13.2 Ma (BALEN et al., 2018b).

Cathodoluminescence images (Fig. 3) show that most zircon grains display a clear magmatic oscillatory zoning, minor sector zoning and thin (a few micrometres) metamorphic overgrowths. Older zircon cores are often identifiable thanks to their CL patterns and by the distribution of melt inclusions

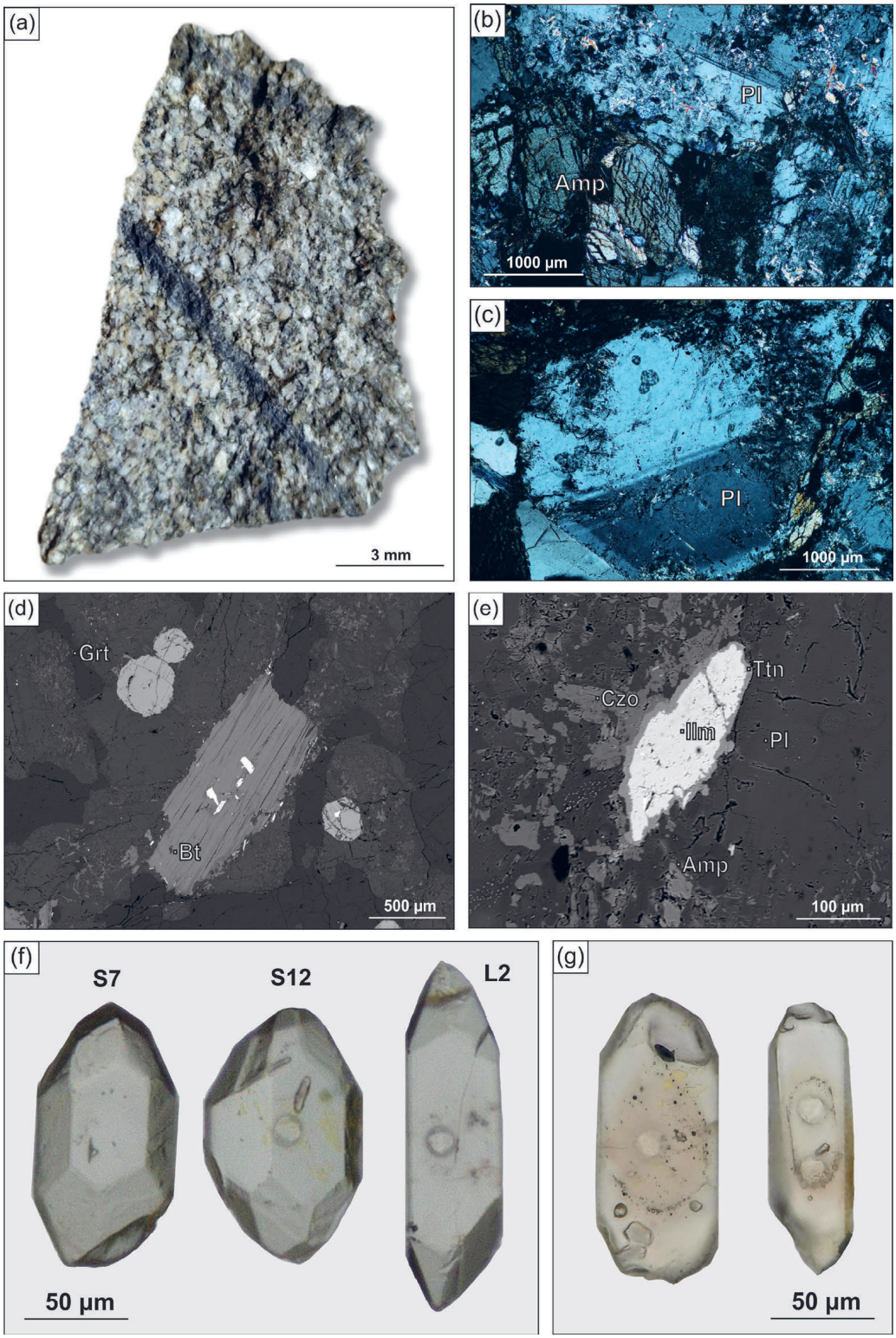

Figure 2. (**a**) Representative sample of the Kutjevo (meta)granitoid with massive rock structure, characterised by prevalent rounded feldspars, weak foliation and dark micaceous bands; (**b**) and (**c**) Cross-polarised transmitted light photomicrographs, showing the major rock-forming minerals and typical rock microfabric; (**d**) and (**e**) Back-scattered electron images of textures and mineral assemblages; (**f**) and (**g**) Plane-polarised transmitted light photomicrographs of separated zircon crystals with different representative forms, where (g) older zircon cores are identified by the distribution of mineral and melt inclusions. Laser ablation pits (15 µm diameter) visible on some grains. Amp – amphibole, Bt – biotite, Czo – clinozoisite, Grt – garnet, Ilm – ilmenite, Pl – plagioclase, Ttn – titanite.

Figure 3. CL images of zircon grains separated from Kutjevo (meta)granitoid sample KU1A, showing internal growth zones and xenocrystic cores. Grains are sorted by increasing $^{206}Pb/^{238}U$ date (± 2 SE uncertainty; the first number next to each spot), while the second number indicates the Th/U ratio. Circles indicate the 35 or 15 µm diameter laser ablation spots, depending on the instrument used for measurements. Analyses with Th/U up to 0.3 are marked in orange and those with Th/U above 0.3 in yellow. Ages with concordance outside the 90–110 % limit are shown in brackets.

in transmitted light images (Fig. 2g). The U content ranges from 43 to 1215 µg/g, and Th/U ratios range from 0.01 to 2.04, with most grains having Th/U ratios higher than 0.1 (median ≈ 0.5), indicating a magmatic origin for these grains.

All the measured zircon grains are shown in Figure 3. In total, 108 analyses were conducted (Table 1), with 10 of them falling outside the 90–110 % concordance limit typically used for provenance (source-to-sink) studies (e.g., SIEGESMUND

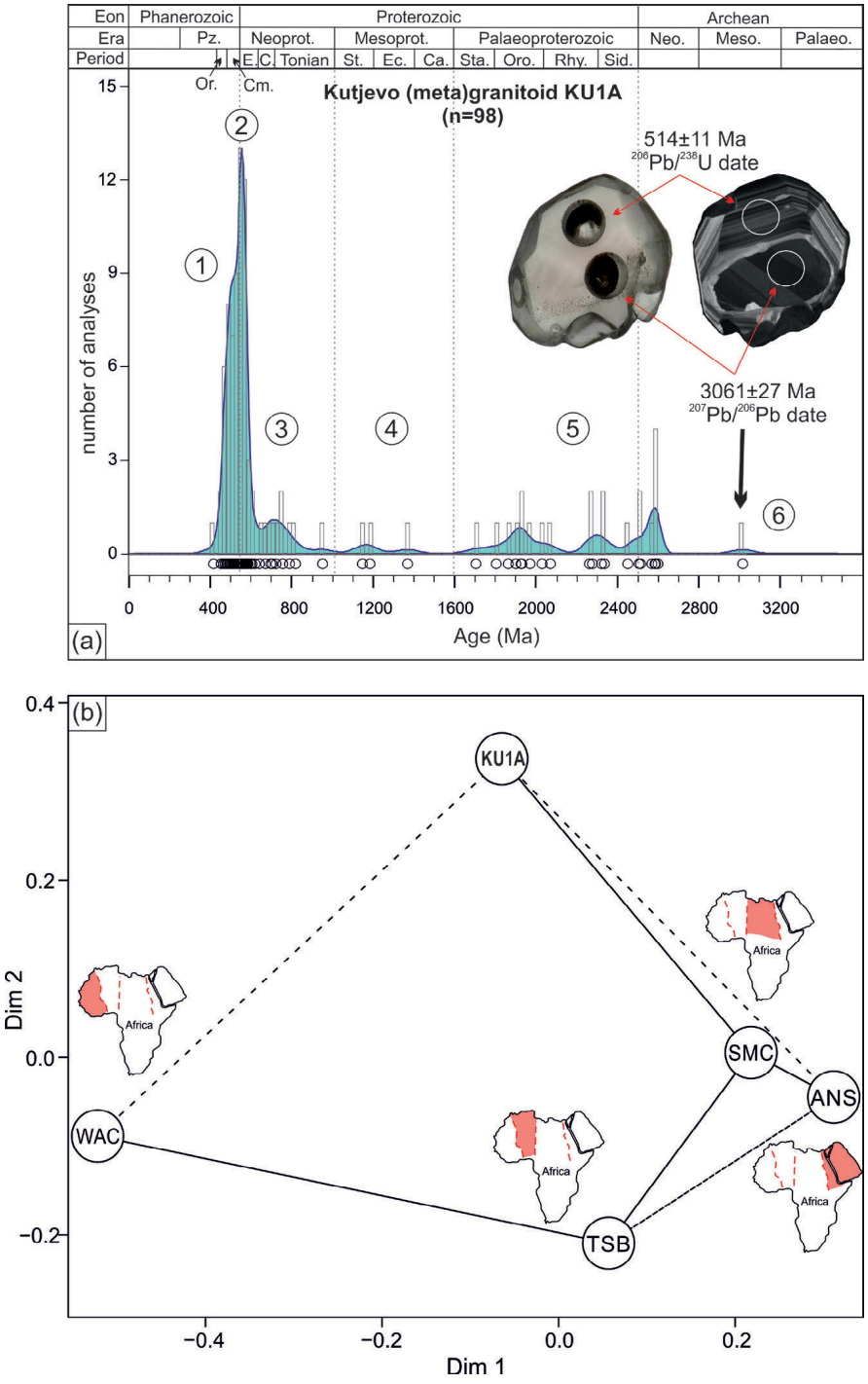

Figure 4. (**a**) Kernel density estimate curves and histograms plotted using DensityPlotter (VERMEESCH, 2012) show age spectra for zircon from the Kutjevo (meta)granitoid (KU1A). The n denotes number of analyses with less than 10 % discordance. Bin and bandwidth are 20 Ma. Main age peaks or areas are indicated with numbers 1 to 6 (see text for an explanation). Inset images (left – plain polarised transmitted light photomicrograph with laser marks, right – CL image) show the oldest zircon in Croatia with positions of measurements: $^{206}Pb/^{238}U$ date in the rim and $^{207}Pb/^{206}Pb$ date in the core, both with ± 2 SE uncertainty. Circles indicate the 35 µm diameter laser ablation spots. Time scale abbreviations: C. – Cryogenian, Ca. – Calymmian, Cm. – Cambrian, E. – Ediacaran, Ec. – Ectasian, Neo. – Neoarchean, Meso. – Mesoarchean, Palaeo. – Palaeoarchean, Pz. – Palaeozoic, Or. – Ordovician, Oro. – Orosirian, Rhy. – Rhyacian, St. – Stenian, Sta. – Statherian, Sid. – Siderian; (**b**) Multidimensional scaling plot of the analysed sample compared to the potential source areas in northern Africa. WAC – West African craton, TSB – Trans-Saharan belt, SMC – Saharan Metacraton, ANS – Arabian–Nubian shield. Data for source areas and the inset image showing the position of the source areas are from ŽÁK et al. (2021). Dim 1 and Dim 2, here calculated using the Kolmogorov–Smirnov test, represent the two principal axes of a 2D "map" designed to show the relative similarity or dissimilarity of zircon age distributions between samples. The solid lines represent the "nearest neighbour" indicating a close affinity with the source, while the dashed lines represent a loose connection ("second closest neighbour").

Table 1. Results of LA-ICP-MS measurements on zircon grains from Kutjevo (meta)granitoid sample (KU1A). Individual elemental concentrations (U, Th, Pb), isotopic ratios and $^{206}Pb/^{238}U$, $^{207}Pb/^{235}U$ and $^{208}Pb/^{232}Th$ dates are reported. The elemental concentration of Pb refers to the sum of all Pb isotopes. Measurements with discordance greater than ±10 % are marked in grey; bold indicates the oldest zircon ($^{207}Pb/^{206}Pb$ date=3061 ± 27 Ma core and its rim) date reported in Croatia so far. ρTW is error correlation of the ratios for a Tera-Wasserburg diagram. Dates are assigned to different chronostratigraphic units according to COHEN et al. (2025).

										Isotopic ratios												Age (Ma)									
Grain point	Spot size (µm)	U (µg/g)	±	Th (µg/g)	±	Th/U	±	Pb (µg/g)	±	$^{207}Pb/^{235}U$	±	$^{206}Pb/^{238}U$	±	r	$^{238}U/^{206}Pb$	±	$^{207}Pb/^{206}Pb$	±	ρTW	$^{208}Pb/^{232}Th$	±	$^{206}Pb/^{238}U$	±	$^{207}Pb/^{235}U$	±	$^{207}Pb/^{206}Pb$	±	% Conc.	$^{208}Pb/^{232}Th$	±	Chronostratigraphic unit
#34	35	867	60	68	7	0.08	0.01	21	2	0.4737	0.0099	0.0551	0.0009	0.55	18.1357	0.3092	0.0627	0.0014	0.23	0.0391	0.0014	346	6	393	7	687	47	88	775	27	
#102	15	2157	43	4080	180	1.89	0.09	6220	200	0.5410	0.0170	0.0600	0.0014	0.98	16.6667	0.3889	0.0654	0.0007	-0.74	0.0138	0.0008	376	9	438	11	785	22	86	277	17	
#106	15	1625	26	965	48	0.59	0.03	2590	120	1.1000	0.0360	0.0626	0.0020	0.63	15.9744	0.5104	0.1277	0.0031	0.29	0.0246	0.0021	391	12	752	17	2060	43	52	490	42	
#20	35	632	15	142	17	0.22	0.03	23	1	0.5810	0.0170	0.0660	0.0018	0.91	15.1515	0.4132	0.0636	0.0012	0.06	0.0302	0.0028	412	11	463	11	719	41	89	598	55	
#30	35	666	11	231	4	0.35	0.01	49	1	0.5590	0.0110	0.0664	0.0011	0.77	15.0625	0.2496	0.0612	0.0012	0.25	0.0232	0.0004	414	7	450	7	641	40	92	463	8	Devonian
#27	35	281	25	63	8	0.22	0.03	18	2	0.6420	0.0170	0.0705	0.0014	0.31	14.1844	0.2817	0.0659	0.0017	0.38	0.0319	0.0007	439	8	502	11	786	52	88	634	13	
#7	35	370	6	56	6	0.15	0.02	13	1	0.5770	0.0130	0.0725	0.0013	0.71	13.7931	0.2473	0.0578	0.0012	0.12	0.0268	0.0015	451	8	462	8	510	46	98	534	30	Ordovician
#94	15	900	15	340	9	0.38	0.01	1046	24	0.6125	0.0100	0.0726	0.0010	0.76	13.7684	0.1896	0.0613	0.0005	0.05	0.0276	0.0013	452	6	485	7	648	18	93	550	25	Ordovician
#28	35	723	73	249	32	0.34	0.06	53	7	0.6034	0.0110	0.0749	0.0010	0.35	13.3583	0.1784	0.0586	0.0012	0.26	0.0247	0.0007	465	6	479	7	542	44	97	492	13	Ordovician
#3	35	598	31	148	6	0.25	0.02	34	1	0.6142	0.0110	0.0755	0.0010	0.35	13.2538	0.1686	0.0591	0.0012	0.31	0.0244	0.0004	469	6	486	7	560	44	97	488	8	Ordovician
#4	35	684	42	225	16	0.33	0.03	50	3	0.6008	0.0100	0.0756	0.0011	0.50	13.2205	0.1923	0.0576	0.0011	0.28	0.0239	0.0004	470	6	477	7	511	42	98	477	8	Ordovician
#79	15	647	40	339	18	0.52	0.04	838	43	0.6103	0.0080	0.0758	0.0007	0.41	13.1891	0.1148	0.0583	0.0006	0.14	0.0222	0.0010	471	4	484	5	538	22	97	443	20	Ordovician
#15	35	491	18	153	4	0.31	0.01	36	1	0.6210	0.0130	0.0760	0.0011	0.62	13.1666	0.1907	0.0590	0.0012	0.08	0.0246	0.0006	472	7	489	8	560	44	96	491	12	Ordovician
#17	35	304	30	79	9	0.26	0.04	18	2	0.6570	0.0160	0.0770	0.0012	0.21	12.9955	0.2027	0.0613	0.0016	0.35	0.0270	0.0010	478	7	511	10	639	54	93	539	19	Ordovician
#56	15	557	11	4	1	0.01	0.00	14	1	0.6107	0.0080	0.0774	0.0006	0.54	12.9283	0.1070	0.0574	0.0007	-0.24	0.0450	0.0190	480	4	484	5	504	24	99	840	350	Ordovician
#22	35	507	19	136	5	0.27	0.01	30	1	0.6231	0.0120	0.0785	0.0011	0.51	12.7437	0.1786	0.0574	0.0011	0.24	0.0243	0.0005	487	6	491	8	499	43	99	485	9	Ordovician
#9	35	365	9	90	1	0.25	0.01	21	0	0.6298	0.0110	0.0795	0.0010	0.41	12.5802	0.1535	0.0572	0.0011	0.24	0.0245	0.0004	493	6	495	7	491	44	100	489	8	Cambrian
#19	35	425	24	177	11	0.42	0.03	39	2	0.6269	0.0110	0.0795	0.0010	0.32	12.5770	0.1534	0.0570	0.0012	0.33	0.0240	0.0004	493	6	494	7	491	47	100	479	8	Cambrian
#14	35	391	17	153	7	0.39	0.03	37	2	0.6356	0.0120	0.0796	0.0011	0.56	12.5676	0.1737	0.0580	0.0011	0.24	0.0252	0.0004	494	7	499	7	521	44	99	502	8	Cambrian
#24	35	729	58	230	23	0.32	0.04	52	5	0.6325	0.0120	0.0800	0.0011	0.63	12.5016	0.1719	0.0573	0.0011	0.16	0.0250	0.0004	496	7	497	7	496	42	100	499	8	Cambrian
#6	35	272	17	57	5	0.21	0.02	14	1	0.6640	0.0130	0.0802	0.0010	0.18	12.4704	0.1493	0.0603	0.0014	0.34	0.0294	0.0012	497	6	517	8	597	49	96	585	23	Cambrian
#35	35	277	22	68	7	0.25	0.03	15	2	0.6330	0.0150	0.0803	0.0013	0.38	12.4533	0.2016	0.0568	0.0014	0.24	0.0259	0.0007	498	8	497	10	470	54	100	518	13	Cambrian
#74	15	515	11	423	18	0.82	0.04	1219	35	0.6452	0.0100	0.0812	0.0008	0.68	12.3183	0.1244	0.0579	0.0006	-0.15	0.0253	0.0014	503	5	505	6	521	24	100	505	28	Cambrian
#10	35	373	30	134	16	0.36	0.05	32	4	0.6460	0.0130	0.0815	0.0010	0.41	12.2730	0.1491	0.0576	0.0013	0.19	0.0258	0.0005	505	6	505	8	503	48	100	514	10	Cambrian
#33	35	500	40	106	16	0.21	0.04	24	3	0.6530	0.0210	0.0823	0.0024	0.76	12.1507	0.3543	0.0579	0.0014	0.34	0.0277	0.0008	510	15	509	13	512	54	100	552	16	Cambrian
#31	35	361	10	79	2	0.22	0.01	17	0	0.6538	0.0120	0.0824	0.0012	0.53	12.1315	0.1766	0.0572	0.0012	0.30	0.0254	0.0007	511	7	510	8	494	45	100	507	14	Cambrian
#83	15	272	16	196	19	0.72	0.08	546	52	0.6700	0.0150	0.0829	0.0008	0.19	12.0627	0.1193	0.0586	0.0012	0.08	0.0249	0.0012	513	5	520	9	556	50	99	496	23	Cambrian

Grain point	Spot size (μm)	U (μg/g)	±	Th (μg/g)	±	Th/U	±	Pb (μg/g)	±	Isotopic ratios $^{207}Pb/^{235}U$	±	$^{206}Pb/^{238}U$	±	r	$^{238}U/^{206}Pb$	±	$^{207}Pb/^{206}Pb$	±	ρTW	$^{208}Pb/^{232}Th$	±	Age (Ma) $^{206}Pb/^{238}U$	±	$^{207}Pb/^{235}U$	±	$^{207}Pb/^{206}Pb$	±	% Conc.	$^{208}Pb/^{232}Th$	±	Chronostratigraphic unit
#18	35	288	10	86	2	0.30	0.01	20	1	0.6530	0.0270	0.0831	0.0019	0.56	12.0337	0.2751	0.0581	0.0024	0.12	0.0266	0.0007	514	11	509	17	511	89	101	530	14	Cambrian
#65	15	266	3	109	2	0.41	0.01	298	5	0.6680	0.0130	0.0832	0.0009	0.59	12.0250	0.1244	0.0583	0.0009	-0.20	0.0246	0.0012	515	5	519	8	533	33	99	492	23	Cambrian
#97	15	96	3	46	2	0.47	0.03	125	6	0.6850	0.0190	0.0840	0.0011	0.23	11.9104	0.1560	0.0590	0.0016	0.25	0.0245	0.0013	520	7	529	11	554	57	98	488	25	Cambrian
#26	35	366	9	44	3	0.12	0.01	15	1	0.7780	0.0170	0.0842	0.0016	0.65	11.8765	0.2257	0.0672	0.0014	0.37	0.0438	0.0029	521	10	584	9	839	43	89	863	55	
#95	15	244	2	95	1	0.39	0.01	260	4	0.6730	0.0130	0.0845	0.0009	0.48	11.8315	0.1218	0.0578	0.0009	-0.05	0.0245	0.0012	523	5	523	8	515	34	100	489	23	Cambrian
#44	15	128	3	91	1	0.71	0.02	250	4	0.7120	0.0140	0.0846	0.0009	0.37	11.8259	0.1231	0.0609	0.0010	0.14	0.0247	0.0012	523	5	545	8	628	36	96	493	23	Cambrian
#80	15	158	6	150	4	0.95	0.04	435	16	0.6960	0.0160	0.0857	0.0009	0.81	11.6659	0.1225	0.0589	0.0012	-0.62	0.0257	0.0012	530	5	536	10	554	46	99	513	24	Cambrian
#99	15	140	5	59	2	0.42	0.02	163	6	0.6950	0.0180	0.0858	0.0010	0.81	11.6618	0.1360	0.0587	0.0012	-0.53	0.0249	0.0013	530	6	535	11	546	47	99	497	25	Cambrian
#66	15	144	3	83	2	0.58	0.02	239	7	0.6970	0.0170	0.0859	0.0010	0.70	11.6469	0.1302	0.0588	0.0011	-0.49	0.0257	0.0012	531	6	536	10	551	44	99	514	25	Cambrian
#101	15	383	6	392	10	1.02	0.03	1230	37	0.7940	0.0220	0.0859	0.0010	0.59	11.6428	0.1328	0.0669	0.0015	-0.31	0.0279	0.0013	531	6	592	12	825	46	90	557	26	Cambrian
#41	15	404	28	371	53	0.92	0.15	990	140	0.6990	0.0120	0.0864	0.0009	0.44	11.5714	0.1138	0.0586	0.0008	0.00	0.0242	0.0011	534	5	538	7	548	30	99	483	22	Cambrian
#108	15	494	21	211	8	0.43	0.02	631	24	0.7096	0.0110	0.0871	0.0009	0.75	11.4784	0.1212	0.0591	0.0006	-0.49	0.0267	0.0012	539	6	544	7	566	22	99	532	24	Cambrian
#98	15	130	4	191	5	1.46	0.06	532	14	0.7150	0.0160	0.0874	0.0010	0.25	11.4430	0.1270	0.0594	0.0013	0.16	0.0249	0.0012	540	6	547	10	571	46	99	497	23	Cambrian
#32	35	106	2	54	3	0.51	0.03	14	1	0.7000	0.0180	0.0876	0.0013	0.24	11.4155	0.1694	0.0579	0.0016	0.29	0.0291	0.0007	541	8	537	11	499	61	101	580	13	Ediacaran
#73	15	144	2	101	2	0.71	0.01	286	6	0.7110	0.0150	0.0880	0.0009	0.28	11.3675	0.1202	0.0586	0.0011	0.11	0.0252	0.0012	544	6	545	9	552	40	100	502	24	Ediacaran
#64	15	480	6	193	13	0.40	0.03	663	39	0.7156	0.0097	0.0890	0.0008	0.57	11.2322	0.1047	0.0583	0.0006	0.01	0.0312	0.0015	550	5	548	6	537	21	100	621	29	Ediacaran
#21	35	278	13	273	16	0.98	0.07	63	2	0.7390	0.0190	0.0891	0.0018	0.75	11.2233	0.2267	0.0604	0.0013	0.30	0.0265	0.0008	550	10	560	11	604	48	98	528	16	Ediacaran
#61	15	446	9	271	5	0.61	0.02	822	20	0.7238	0.0100	0.0892	0.0008	0.42	11.2133	0.1006	0.0588	0.0006	0.11	0.0272	0.0013	551	5	553	6	555	24	100	542	25	Ediacaran
#48	15	613	11	441	13	0.72	0.02	1261	41	0.7213	0.0094	0.0892	0.0008	0.49	11.2057	0.1017	0.0586	0.0006	0.06	0.0257	0.0012	551	5	552	5	550	21	100	513	23	Ediacaran
#38	15	145	2	63	1	0.44	0.01	212	5	0.8050	0.0200	0.0896	0.0009	0.20	11.1607	0.1121	0.0651	0.0015	0.09	0.0301	0.0015	553	5	599	11	766	49	92	599	29	Ediacaran
#67	15	694	13	787	8	1.13	0.02	2452	29	0.7205	0.0082	0.0896	0.0008	0.55	11.1570	0.1033	0.0582	0.0004	0.27	0.0279	0.0013	553	5	551	5	539	16	100	556	25	Ediacaran
#70	15	359	4	339	4	0.94	0.02	954	14	0.7341	0.0097	0.0899	0.0008	0.29	11.1222	0.0977	0.0593	0.0006	0.19	0.0252	0.0012	555	5	560	5	577	21	99	504	23	Ediacaran
#82	15	86	1	171	2	1.98	0.04	499	8	0.7380	0.0230	0.0901	0.0011	0.41	11.1049	0.1357	0.0594	0.0016	-0.10	0.0260	0.0012	556	6	560	13	565	58	99	519	24	Ediacaran
#85	15	72	1	42	1	0.58	0.02	128	4	0.7420	0.0280	0.0901	0.0013	0.34	11.0988	0.1601	0.0597	0.0021	-0.02	0.0275	0.0014	556	7	562	16	583	71	99	549	28	Ediacaran
#39	15	138	2	80	1	0.58	0.01	229	4	0.7390	0.0160	0.0905	0.0009	0.22	11.0461	0.1037	0.0592	0.0011	0.12	0.0256	0.0012	559	5	561	9	567	42	100	511	24	Ediacaran
#92	15	190	2	258	3	1.36	0.02	771	10	0.7308	0.0110	0.0908	0.0011	0.28	11.0120	0.1334	0.0585	0.0009	0.30	0.0267	0.0012	560	6	557	7	541	33	101	533	24	Ediacaran
#58	15	249	4	137	3	0.55	0.01	396	9	0.7340	0.0120	0.0915	0.0008	0.06	10.9314	0.0956	0.0582	0.0008	0.29	0.0261	0.0012	564	5	559	7	532	32	101	520	24	Ediacaran
#37	15	59	1	30	1	0.51	0.02	90	2	0.7390	0.0250	0.0917	0.0018	0.40	10.9051	0.2141	0.0584	0.0018	0.17	0.0275	0.0016	566	10	560	14	525	68	101	549	31	Ediacaran
#1	35	44	2	17	1	0.38	0.03	4	0	0.7430	0.0270	0.0918	0.0014	0.17	10.8933	0.1661	0.0586	0.0021	0.22	0.0285	0.0007	566	9	560	15	499	81	101	567	15	Ediacaran

										Isotopic ratios													Age (Ma)									
Grain point	Spot size (μm)	U (μg/g)	±	Th (μg/g)	±	Th/U	±	Pb (μg/g)	±	$^{207}Pb/^{235}U$	±	$^{206}Pb/^{238}U$	±	r	$^{238}U/^{206}Pb$	±	$^{207}Pb/^{206}Pb$	±	ρTW	$^{208}Pb/^{232}Th$	±	$^{206}Pb/^{238}U$	±	$^{207}Pb/^{235}U$	±	$^{207}Pb/^{206}Pb$	±	% Conc.	$^{208}Pb/^{232}Th$	±	Chronostratigraphic unit
#8	35	284	11	248	10	0.87	0.05	66	2	0.7430	0.0140	0.0923	0.0012	0.45	10.8319	0.1408	0.0584	0.0012	0.29	0.0276	0.0004	569	7	563	8	536	47	101	551	8	Ediacaran
#29	35	77	3	54	2	0.70	0.03	15	0	0.7940	0.0240	0.0927	0.0019	0.29	10.7875	0.2211	0.0621	0.0019	0.26	0.0302	0.0006	571	11	592	14	654	68	97	601	12	Ediacaran
#40	15	56	2	62	1	1.11	0.04	181	4	0.7640	0.0300	0.0929	0.0017	0.53	10.7643	0.1970	0.0593	0.0020	-0.04	0.0261	0.0013	572	10	574	17	555	76	100	520	25	Ediacaran
#62	15	109	3	57	2	0.52	0.02	167	5	0.7630	0.0190	0.0930	0.0013	0.51	10.7527	0.1503	0.0595	0.0012	0.02	0.0264	0.0013	573	8	575	11	586	42	100	526	26	Ediacaran
#5	35	303	5	224	5	0.74	0.02	62	2	0.7850	0.0160	0.0931	0.0013	0.57	10.7411	0.1500	0.0613	0.0013	0.15	0.0289	0.0005	574	8	587	9	639	45	98	575	10	Ediacaran
#46	15	74	1	69	1	0.94	0.02	200	3	0.7680	0.0230	0.0936	0.0013	0.76	10.6838	0.1484	0.0595	0.0014	-0.43	0.0261	0.0013	577	8	577	13	573	52	100	520	26	Ediacaran
#76	15	165	5	34	2	0.21	0.01	109	4	0.7620	0.0160	0.0939	0.0010	0.60	10.6553	0.1079	0.0588	0.0011	-0.36	0.0290	0.0016	578	6	574	9	553	41	101	578	31	Ediacaran
#13	35	96	2	54	1	0.56	0.02	15	0	0.7620	0.0200	0.0941	0.0013	0.37	10.6304	0.1469	0.0589	0.0016	0.16	0.0294	0.0005	579	8	574	12	538	60	101	586	10	Ediacaran
#81	15	676	9	542	6	0.80	0.01	1735	26	0.7757	0.0096	0.0942	0.0009	0.74	10.6168	0.1003	0.0597	0.0004	-0.32	0.0285	0.0013	580	5	583	6	592	16	100	569	26	Ediacaran
#107	15	43	1	42	1	0.97	0.03	130	3	0.7880	0.0290	0.0954	0.0018	0.44	10.4822	0.1978	0.0599	0.0019	0.03	0.0280	0.0016	587	10	588	16	579	70	100	558	31	Ediacaran
#53	15	65	1	57	1	0.87	0.02	173	4	0.8180	0.0250	0.0971	0.0013	0.46	10.2987	0.1379	0.0610	0.0016	-0.07	0.0274	0.0014	598	8	606	14	623	59	99	547	27	Ediacaran
#51	15	412	8	839	25	2.04	0.07	2605	73	0.8185	0.0110	0.0985	0.0010	0.65	10.1564	0.1032	0.0603	0.0006	0.08	0.0279	0.0013	605	6	607	6	611	20	100	556	25	Ediacaran
#36	15	120	4	96	3	0.80	0.04	317	10	0.8340	0.0190	0.1005	0.0012	0.57	9.9502	0.1188	0.0602	0.0011	-0.17	0.0296	0.0014	617	7	615	11	602	39	100	589	27	Ediacaran
#90	15	501	48	302	32	0.60	0.09	1040	100	0.8710	0.0170	0.1045	0.0016	0.80	9.5694	0.1465	0.0607	0.0007	-0.29	0.0313	0.0015	641	9	636	9	626	26	101	624	30	Cryogenian
#55	15	90	1	43	1	0.48	0.01	159	7	0.9970	0.0330	0.1096	0.0015	0.46	9.1241	0.1249	0.0660	0.0020	-0.17	0.0337	0.0020	670	9	700	17	801	66	96	670	39	Cryogenian
#23	35	645	28	187	9	0.29	0.02	62	3	1.4950	0.0830	0.1111	0.0036	0.93	9.0009	0.2917	0.0960	0.0031	-0.70	0.0379	0.0012	678	21	915	36	1532	64	74	751	23	
#72	15	175	8	72	4	0.41	0.03	257	14	0.9990	0.0210	0.1138	0.0011	0.58	8.7881	0.0850	0.0637	0.0011	-0.22	0.0320	0.0016	695	7	703	11	726	35	99	636	31	Cryogenian
#12	35	137	4	136	9	0.99	0.07	48	3	1.0740	0.0340	0.1151	0.0018	0.60	8.6881	0.1359	0.0674	0.0020	-0.19	0.0363	0.0007	702	11	735	16	816	58	96	721	14	Cryogenian
#88	15	286	9	200	7	0.70	0.03	766	28	1.0343	0.0130	0.1184	0.0011	0.70	8.4452	0.0785	0.0634	0.0007	-0.48	0.0343	0.0016	721	6	721	6	717	23	100	683	31	Tonian
#54	15	150	3	67	2	0.45	0.01	277	8	1.1040	0.0210	0.1243	0.0013	0.64	8.0451	0.0841	0.0644	0.0009	-0.25	0.0369	0.0018	755	8	755	10	751	29	100	732	35	Tonian
#2	35	283	9	402	22	1.42	0.09	148	7	1.1720	0.0260	0.1246	0.0027	0.06	8.0257	0.1739	0.0681	0.0021	0.76	0.0395	0.0009	756	15	786	12	851	59	96	783	17	Tonian
#25	35	244	12	57	3	0.23	0.02	23	0	1.8900	0.1100	0.1251	0.0040	0.95	7.9936	0.2556	0.1079	0.0036	-0.75	0.0476	0.0021	759	23	1062	40	1752	59	71	940	41	
#59	15	274	8	158	5	0.58	0.02	700	23	1.1590	0.0210	0.1304	0.0012	0.31	7.6705	0.0706	0.0644	0.0010	0.10	0.0400	0.0019	790	7	781	10	752	33	101	792	37	Tonian
#43	15	328	5	294	3	0.90	0.02	1095	15	1.3060	0.0190	0.1353	0.0013	0.64	7.3915	0.0710	0.0700	0.0007	-0.11	0.0334	0.0015	818	7	848	8	925	19	96	664	30	Tonian
#105	15	916	20	204	6	0.22	0.01	1061	20	2.6500	0.1300	0.1487	0.0042	0.95	6.7250	0.1899	0.1284	0.0033	-0.77	0.0467	0.0024	893	23	1307	37	2067	46	68	922	47	
#60	15	151	3	58	1	0.39	0.01	313	4	1.5640	0.0280	0.1589	0.0018	0.52	6.2933	0.0713	0.0715	0.0010	-0.21	0.0483	0.0023	950	10	956	11	967	29	99	954	45	Tonian
#47	15	121	1	51	1	0.42	0.01	296	4	2.1300	0.0380	0.1949	0.0023	0.55	5.1308	0.0605	0.0794	0.0012	-0.07	0.0529	0.0027	1148	12	1158	12	1178	29	99	1043	51	Stenian
#42	15	90	1	28	1	0.31	0.01	167	3	2.2440	0.0370	0.2015	0.0024	0.29	4.9628	0.0591	0.0808	0.0012	0.37	0.0543	0.0031	1183	13	1194	11	1218	27	99	1069	59	Stenian
#75	15	370	11	160	3	0.43	0.01	1387	26	3.3800	0.1100	0.2369	0.0071	0.99	4.2212	0.1265	0.1033	0.0007	-0.40	0.0775	0.0035	1369	37	1495	26	1684	12	92	1508	66	

Grain point	Spot size (μm)	U (μg/g)	±	Th (μg/g)	±	Th/U	±	Pb (μg/g)	±	Isotopic ratios $^{207}Pb/^{235}U$	±	$^{206}Pb/^{238}U$	±	r	$^{238}U/^{206}Pb$	±	$^{207}Pb/^{206}Pb$	±	ρTW	$^{208}Pb/^{232}Th$	±	Age (Ma) $^{206}Pb/^{238}U$	±	$^{207}Pb/^{235}U$	±	$^{207}Pb/^{206}Pb$	±	% Conc.	$^{208}Pb/^{232}Th$	±	Chronostratigraphic unit
#63	15	476	34	449	47	0.94	0.12	3460	250	5.9000	0.1700	0.2776	0.0067	0.99	3.6023	0.0869	0.1538	0.0010	-0.81	0.0725	0.0040	1578	34	1956	25	2387	12	81	1415	75	
#57	15	155	3	103	2	0.66	0.02	946	21	4.2720	0.0700	0.3025	0.0041	0.40	3.3058	0.0448	0.1024	0.0015	0.41	0.0830	0.0040	1703	20	1688	14	1667	27	101	1612	74	Palaeoproterozoic
#52	15	111	1	78	2	0.71	0.02	752	18	4.9230	0.0700	0.3226	0.0034	0.65	3.0998	0.0327	0.1107	0.0010	0.01	0.0858	0.0040	1802	17	1806	12	1808	17	100	1664	75	Palaeoproterozoic
#87	15	749	14	27	2	0.04	0.00	228	15	6.6900	0.1300	0.3351	0.0059	0.92	2.9842	0.0525	0.1447	0.0011	0.01	0.0795	0.0059	1862	28	2070	17	2282	13	90	1545	110	Palaeoproterozoic
#11	35	1061	45	20	1	0.02	0.00	22	1	7.0500	0.1400	0.3430	0.0060	0.70	2.9155	0.0510	0.1494	0.0029	0.34	0.1167	0.0027	1900	29	2115	19	2336	34	90	2230	49	Palaeoproterozoic
#49	15	214	14	73	4	0.34	0.03	752	34	6.0660	0.0740	0.3481	0.0039	0.83	2.8727	0.0322	0.1264	0.0007	0.22	0.0933	0.0044	1925	19	1985	11	2047	10	97	1802	82	Palaeoproterozoic
#68	15	383	12	137	2	0.36	0.01	1631	39	6.9600	0.3100	0.3490	0.0120	0.99	2.8653	0.0985	0.1436	0.0017	-0.93	0.1061	0.0049	1928	60	2095	42	2269	20	92	2037	90	Palaeoproterozoic
#50	15	194	4	109	2	0.56	0.02	1135	23	6.1680	0.0670	0.3572	0.0031	0.71	2.7996	0.0243	0.1252	0.0007	0.00	0.0938	0.0043	1969	15	2000	10	2030	11	98	1812	80	Palaeoproterozoic
#84	15	452	6	44	2	0.10	0.00	535	36	6.7900	0.2500	0.3700	0.0066	0.98	2.7027	0.0482	0.1325	0.0026	-0.93	0.1076	0.0061	2029	31	2078	32	2125	34	98	2064	110	Palaeoproterozoic
#103	15	169	3	73	2	0.43	0.01	810	17	6.8350	0.0780	0.3784	0.0037	0.74	2.6427	0.0258	0.1312	0.0009	0.05	0.0985	0.0046	2069	17	2091	11	2113	11	99	1899	85	Palaeoproterozoic
#91	15	462	3	98	7	0.21	0.02	1359	99	9.2500	0.2400	0.4204	0.0063	0.97	2.3787	0.0356	0.1592	0.0020	-0.86	0.1237	0.0058	2262	29	2359	24	2444	22	96	2358	100	Palaeoproterozoic
#78	15	98	2	23	1	0.24	0.01	337	5	10.7300	0.1500	0.4239	0.0049	0.85	2.3590	0.0273	0.1835	0.0013	-0.17	0.1321	0.0078	2278	22	2499	13	2684	12	91	2504	140	Palaeoproterozoic
#104	15	147	2	105	1	0.71	0.01	1363	13	10.9200	0.1400	0.4335	0.0049	0.88	2.3068	0.0261	0.1829	0.0009	0.02	0.1161	0.0054	2321	22	2516	12	2678	8	92	2220	97	Palaeoproterozoic
#89	15	1215	17	886	15	0.73	0.02	11570	190	10.0560	0.0980	0.4370	0.0039	0.95	2.2883	0.0204	0.1669	0.0005	0.05	0.1167	0.0054	2337	18	2440	9	2526	5	96	2230	98	Palaeoproterozoic
#69	15	139	2	74	1	0.53	0.01	998	11	10.6600	0.1400	0.4626	0.0042	0.75	2.1617	0.0196	0.1670	0.0012	-0.22	0.1206	0.0057	2451	19	2495	11	2527	12	98	2301	100	Palaeoproterozoic
#93	15	385	8	117	3	0.30	0.01	1688	37	12.0120	0.1400	0.4746	0.0050	0.95	2.1070	0.0222	0.1836	0.0007	-0.01	0.1280	0.0060	2504	22	2605	11	2684	7	96	2434	110	Archean
#45	15	171	2	77	1	0.45	0.01	1035	11	12.0500	0.1300	0.4767	0.0042	0.80	2.0978	0.0185	0.1832	0.0009	-0.12	0.1200	0.0056	2513	18	2609	9	2681	8	96	2297	110	Archean
#77	15	145	2	43	1	0.30	0.01	626	9	12.0300	0.1600	0.4894	0.0055	0.92	2.0433	0.0230	0.1783	0.0010	-0.32	0.1316	0.0067	2568	24	2606	12	2636	10	99	2498	120	Archean
#100	15	345	7	254	7	0.74	0.03	3584	94	12.2640	0.1300	0.4921	0.0047	0.90	2.0321	0.0194	0.1808	0.0008	-0.06	0.1260	0.0057	2582	22	2625	10	2659	7	98	2399	100	Archean
#96	15	303	5	140	2	0.46	0.01	2060	34	12.5490	0.1300	0.4935	0.0046	0.90	2.0263	0.0189	0.1844	0.0008	-0.01	0.1312	0.0061	2586	20	2646	10	2692	7	98	2492	110	Archean
#86	15	273	14	145	10	0.53	0.05	2080	130	13.2600	0.1400	0.4935	0.0043	0.58	2.0263	0.0177	0.1946	0.0013	0.30	0.1293	0.0060	2588	20	2698	10	2781	11	96	2458	110	Archean
#71	15	114	1	56	1	0.49	0.01	792	9	12.2900	0.1600	0.4961	0.0055	0.84	2.0157	0.0223	0.1796	0.0012	-0.08	0.1255	0.0060	2597	24	2626	13	2648	11	99	2390	110	Archean
#16	**35**	**249**	**9**	**188**	**6**	**0.75**	**0.03**	**281**	**7**	**19.0600**	**0.2800**	**0.5957**	**0.0072**	**0.82**	**1.6787**	**0.0203**	**0.2315**	**0.0039**	**0.38**	**0.1613**	**0.0022**	**3014**	**30**	**3044**	**14**	**3061**	**27**	**99**	**3022**	**38**	**Archean**

et al., 2018, 2021, 2023; MEINHOLD et al., 2021; VESELÁ et al., 2022). We use the same concordance limit for $^{206}Pb/^{238}U$ dates, although most of our data fall between 96 % and 101 % concordance. For older cores that are reported individually, $^{207}Pb/^{206}Pb$ dates are also provided (Fig. 4, Table 1), because the concordia curve flattens at older ages (>1 Ga), making the $^{207}Pb/^{206}Pb$ ratio more robust and better defined for these dates.

The Palaeozoic record comprises 34 dates: 23 Cambrian, 10 Ordovician and one Devonian. The Neoproterozoic contains 39 dates, dominated by 29 Ediacaran (E) results. Tonian (T) and Stenian (S) dates are relatively rare, represented by six and two dates, respectively. Including four Cryogenian (C) dates, the E/(C+T+S) age ratio is approximately 2.5. Fourteen dates are recorded for the Palaeoproterozoic (PP), resulting in a characteristic ratio of (T+S)/PP ≈ 0.6. Older (Archean) dates, including the oldest zircon core, are recorded in eight spots (Table 1).

The age clusters are shown as peaks in the kernel density estimate (KDE) diagram (Fig. 4a), based on the data from 98 analyses. There is a prominent Lower Palaeozoic/Ediacaran asymmetric peak comprising about 64 % of all concordant analyses, a significantly weaker mainly Neoproterozoic (C+T+S; ≈ 12 %) "Pan-African" hump, dispersed and rare Mesoproterozoic dates (a gap between ≈ 0.8–1.6 Ga) and a significant number of Palaeoproterozoic dates (≈ 14 % of concordant analyses) between 1.6 and 2.5 Ga. Archean dates account for ≈ 8 % of analyses. The oldest record, mainly from the xenocrystic cores, includes 32 concordant dates older than 700 Ma. The visually asymmetric youngest peak (Fig. 4a) can be subdivided into two peaks by separating dates with Th/U ratios lower and higher than 0.3. The younger cluster, comprising 12 analyses with Th/U ratios up to 0.3 (Fig. 5 left inset), yields an age of 497.9 ± 1.9 | 6.8 Ma (age ± 2SE uncertainty | total 2SE including systematic uncertainties), while the main magmatic group (47 analyses, with 0.3 < Th/U < 1.5, Palaeozoic/Ediacaran ages <600 Ma to exclude a Pan-African contribution) has an age of 535.3 ± 0.9 | 7.1 Ma (Fig. 5 right inset). By carefully selecting only analyses with Th/U ratios representative of magmatic zircon growth showing a time gap between individual analyses of less than ≈ 20 Ma, influences of Pan-African and Cenerian orogenies on the main magmatic group are minimized. However, an effect of the mentioned orogenies, particularly of the temporally close Cenerian orogeny, cannot be completely avoided, and therefore, the calculated age of 535.3 ± 0.9 | 7.1 Ma should be treated as a minimum crystallisation age estimate.

To resolve similarities with the old cratonic dates, the multi-dimensional scaling (MDS) approach is applied using the Kolmogorov–Smirnov (K–S) test as a (dis)similarity measure (Fig. 4b). This statistical method allows comparison of multiple complex samples within a single diagram. Comparison with potential sources in a present-day northern Africa (West African craton, Trans-Saharan belt, Saharan Metacraton, and Arabian–Nubian shield), using data compiled in ŽÁK et al. (2021), reveals "nearest neighbour" (solid line) similarity of zircon grains from the Kutjevo (meta)granitoid sample with the Saharan Metacraton as a potential source area, and "second closest neighbour" (dashed line) similarity with the Arabian-Nubian shield and also the West African craton.

The Archean dates obtained are related to xenocrystic cores derived from ancient cratonic rocks that contain old zircon grains which survived younger igneous and metamorphic events. The $^{207}Pb/^{206}Pb$ date of 3061 ± 27 Ma represents the crystallisation age of the oldest robustly dated mineral in Croatia, while the main age cluster at ≈ 535 Ma represents the crystallisation age of the oldest igneous rock formation in Croatia.

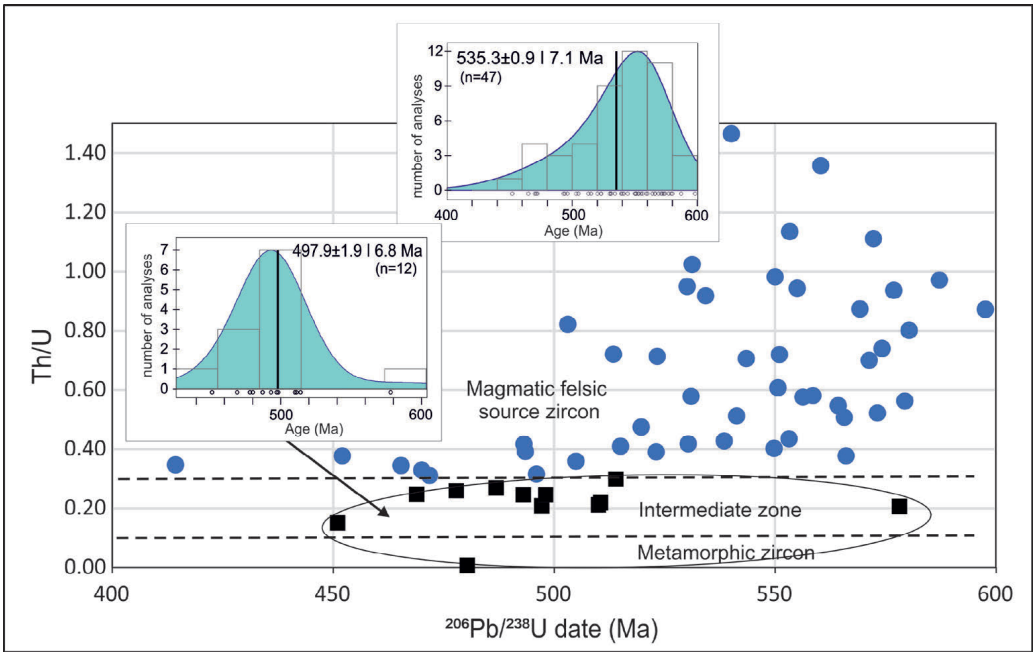

Figure 5. Zircon Th/U ratio versus $^{206}Pb/^{238}U$ date diagram for zircon from the Kutjevo (meta)granitoid (KU1A). The insets show KDE curves and histograms with ages obtained for spots with Th/U up to 0.3 (metamorphic and intermediate zircon) interpreted as indicators of a Cenerian orogeny contribution (left) and Th/U > 0.3 for magmatic zircon from felsic sources, interpreted as the crystallisation age during the Cadomian orogeny (right). The age is given in the format: age ± 2SE uncertainty | total 2SE including systematic uncertainties; n = number of analyses. For Cadomian orogeny zircon dates, a maximum of 600 Ma is set to avoid overlap and influence from the Pan-African orogeny (see text for explanation).

5. DISCUSSION

The commonly accepted view is that the oldest rocks incorporated in the crystalline basement of the Alpine chain originated from the Afro-Arabian sector of the northern Gondwana margin, which was part of the Avalonian-Cadomian belt (e.g., SIEGESMUND et al., 2021; NEUBAUER et al., 2002, 2020). The provenance signal from the pre-orogenic detrital zircon record of the Peri-Gondwanan crust reveals three distinct zircon provenance areas: Avalonia north of the Rheic Ocean, and two contrasting super-fan systems along the vast Peri-Gondwanan shelf – West African and East African–Arabian (STEPHAN et al., 2019a, b). The metasedimentary rocks of the Adriatic Plate belong to the East African–Arabian zircon province, whereas the Alpine basement units related to the European plate display the signatures of the West African zircon provinces; both belong to the peri-Gondwana margin (STEPHAN et al., 2019a, b; SIEGESMUND et al., 2023). There are numerous provenance studies that record Cadomian/Avalonian basement precursors in the Carpathians (e.g., PUTIŠ et al., 2008; BALINTONI & BALICA, 2013; STOICA et al., 2016; BURDA et al., 2021; KOHÚT et al., 2022), Alps (e.g., HAAS et al., 2020; CHANG et al., 2021; NEUBAUER et al., 2020, 2022; VESELÁ et al., 2022; SIEGESMUND et al., 2018, 2021; FINGER & RIEGLER, 2023; KLUG et al., 2025), Variscides and pre-Variscides (e.g., SPAHIĆ et al., 2025; ZEH et al., 2025; FINGER & RIEGLER, 2025). According to FINGER & RIEGLER (2023, 2025), the Cenerian (Ediacaran–Ordovician) and Cadomian (Ediacaran–Cambrian) orogens are two distinct and spatially separated coastal orogens within the Avalonian–Cadomian belt, as defined by NANCE et al. (2008, 2010). The Cenerian orogen, an Alaskan-type orogen, was located farther to the east near the Arabian–Nubian shield, from which it inherited a characteristic Tonian/Stenian detrital zircon signal (1.2–0.8 Ga), while the Cadomian orogen, considered as an Andean-type orogen, originally laid in front of the Saharan Metacraton (ZURBRIGGEN, 2015, 2017; SIEGESMUND et al., 2023; FINGER & RIEGLER, 2023, 2025). The distribution of U-Pb zircon ages of Peri-Gondwana Cambro–Ordovician magmatic rocks shows that bimodal and peralkaline Cambrian magmatism occurred in the West African Zircon Province, whereas calc-alkaline and peraluminous Ordovician magmatism predominated in the East African–Arabian Zircon Province (STEPHAN et al., 2019b).

Since the Ediacaran–Cambrian dates are present in all peri-Gondwanan terranes and likely represent Cadomian volcanic arc-derived material, they have rather limited palaeogeographic significance (ŽÁK et al., 2021). In contrast, older cratonic dates are much more significant for this purpose, but direct similarity is often obscured by numerous data from various sources. The KDE curves and histograms (Fig. 4a) show a zircon age spectrum for the Kutjevo (meta)granitoid sample (KU1A), which can be visually divided into six parts: a dominant and asymmetric (1) Early Palaeozoic / (2) Ediacaran peak; (3) a Pan-African Neoproterozoic hump; (4) a "gap" with sporadic Mesoproterozoic ages; (5) a Palaeoproterozoic range; and (6) Archean dates with the oldest zircon core.

The youngest prominent Early Palaeozoic / Late Neoproterozoic asymmetric peak indicates the presence of Cenerian and Cadomian ages, confirming North Gondwanan inheritance. There is abundant evidence for late Ediacaran to early Palaeozoic, Cadomian to Cenerian orogenic processes in the European pre-Mesozoic basement (e.g., ZURBRIGGEN, 2015, 2017; BURDA et al., 2021; PETRIK et al., 2024; KLUG et al., 2025; SZEMERÉDI et al., 2025). The basement mainly consists of Pan-African metasedimentary and subordinate metaigneous rocks (SIEGESMUND et al., 2021), including Cambrian–Ordovician metagranitoids, which are significant products of ancient orogenic processes. Although surface exposures of these rocks are relatively common (to the extent that relicts can be common), their recognition and genetic details are often obscured by Variscan and/or Alpine metamorphic overprints.

The recognition and significance of Ordovician metagranitoids in the Alps have come into focus, especially in the past decade (ZURBRIGGEN, 2015, 2017), within a model in which they are products of the Cenerian orogeny. Petrogenetic conditions, particularly the temperatures developed during such events, along with zircon solubility in the melt, dictate whether these rocks may preserve and inherit old zircon cores (as seeds for later overgrowth), and provide an important genetic link between the crystalline basement rocks of the Pannonian Basin and the detrital (meta)sedimentary record produced by erosion of ancient Gondwana-related cratons. For the petrogenesis of Ordovician metagranitoids, the model for the Ordovician orogeny in the Alps proposed by ZURBRIGGEN (2015) invokes the erosion of the late Pan-African belts, which produced large volumes of clastic sedimentary rocks (greywackes and pelites) deposited into the trenches of subduction zones along the northern rim of Gondwana. There, they formed extensive subduction and accretion complexes. Furthermore, due to the large sediment input, subduction retreated and mantle-derived magmas intruded the base of the metasedimentary units, which, under conditions of substantial anatexis, produced intrusions and extrusions of syntectonic peraluminous magmas, the compositions of which correspond to the mean compositions of subducted sedimentary rocks. This model resembles the present-day Alaskan-type orogen and indicates sediment delivery from northern Gondwana by the (at that time South Polar) ice sheet, which, during transport, preserved debris from further physical and chemical weathering. Transport encompassed detritus from the entire continental hinterland, allowing incorporation (but also almost complete recycling) of very old material. This explains why older (e.g., Precambrian) basement crystalline units are not found in the accretionary complexes themselves (e.g., in the Alps).

However, zircon cores (xenocrysts) that represent inherited grains may preserve ancient ages and geochemical information from ancient hinterland source rocks. Such an Early Palaeozoic event, which culminated in the Ordovician and led to the formation of several hundred kilometre wide cratonised subduction and accretion complexes hosting peraluminous (fore)arcs, is related to the Cenerian orogeny (ZURBRIGGEN, 2015, 2017, 2020). Nevertheless, sediment supply from the Gondwana super-fan system sourced from the East African–Arabian region (MEINHOLD et al., 2013, 2021) or from changing drain-

age systems from the West African craton (BRADLEY et al., 2022; PASTORE et al., 2021, 2023; BORREGO et al., 2026) as a mechanism that delivered terrigenous sediments over vast periods of time before the Neoproterozoic cannot be excluded.

5.1. Cenerian ages

Cenerian ages (group 1) are potentially hidden among 33 Cambrian and Ordovician ages recorded in different spots (Fig. 3). Examining the prominent Early Palaeozoic / Late Neoproterozoic asymmetric peak (Fig. 4a) and the Th/U ratios (Fig. 5), the Early Palaeozoic ages associated with Th/U up to 0.3 can be assigned to a thermal (?) overprint on the main crystallisation event (and age) of the granitoid, fitting well within the Cenerian orogeny. The age of 497.9 ± 1.9 | 6.8 Ma coincides with the igneous crystallisation of an S-type granite from western Papuk, which has a Cambrian–(Ordovician) crystallisation age of 498.9 ± 6.9 Ma (GALLHOFER et al., 2026).

5.2. Cadomian ages

The Cadomian orogen (ca. 600–520 Ma) is almost universally recorded in European basement realms. It began to develop with the onset of subduction along the northern Gondwana margin and overlaps with the final stages of the Pan-African orogeny (ca. 650–550 Ma), which assembled Western Gondwana (SIEGESMUND et al., 2023). The main limitation is that late Pan-African processes temporally overlap with the early stages of the Cadomian orogeny making it difficult to distinguish between the two sources. Therefore, the Th/U ratio was the main criterion for distinguishing the Cenerian (Th/U $\leq$ 0.3) event from the Cadomian (0.3 < Th/U < 1.5) event, as Th/U values up to 0.3 are more typical of metamorphic and intermediate zircons (Fig. 5), while higher values indicate magmatic zircons. To separate the Cadomian from Pan-African events, we retain magmatic felsic source zircons (0.3 < Th/U < 1.5) and dates younger than 600 Ma, as we observed a gap of approximately 20 Ma towards older ages.

Cambrian and Ediacaran ages (group 2) obtained from oscillatory-zoned magmatic growth zones are predominant (ca. 52 % of all measurements) and therefore, are interpreted to yield the crystallisation age of the host rock. The obtained age of 535.3 ± 0.9 | 7.1 Ma overlaps within uncertainty the age previously reported by BALEN et al. (2018b), who report a $^{206}Pb/^{238}U$ zircon age of 554 ± 13.2 Ma from the same lithology. This identifies the Kutjevo (meta)granitoid as the, so far, oldest robustly dated rock in Croatia.

5.3. Neoproterozoic – "Pan-African hump" (≈ 650−800 Ma)

Ediacaran ages (29 analyses) comprise both a Cadomian and Pan-African contribution (group 3). The lack of a significant population of Late Stenian to Tonian zircon – characteristic of the northeastern Saharan Metacraton and the northern Arabian–Nubian shield – as a source for the metasedimentary sequence, shifts the source area more toward the northwestern margin of the Saharan Metacraton, rather than the West African craton (e.g., ORIOLO et al., 2021). This is supported by the Armorican rocks derived from those regions, which display a distinct Mesoproterozoic gap in their detrital zircon age spectra from 1.6 to 1.0 Ga (LINDNER et al., 2021a, b; FINGER & RIEGLER, 2023). The Cryogenian+Tonian+Stenian zircon population, with characteristic ratio E/(C+T+S) ≈ 2.5, supports the Cadomian event. The Saharan Metacraton was probably the main source of these zircon grains, although a minor contribution of the West African craton and Arabian–Nubian shield is not completely excluded, as MDS analysis point to those areas as potential distant source (Fig. 4b).

5.4. Mesoproterozoic gap

The frequency ratio of Palaeoproterozoic zircon (1.6–2.5 Ga) to Tonian/Stenian zircon (0.8–1.2 Ga) in the (meta)granitoid of the Kutjevo area ((T+S)/PP ≈ 0.6) shows a predominance of Palaeoproterozoic zircon (group 5) and a Mesoproterozoic gap (group 4). Based on this, Mesoproterozoic and Palaeoproterozoic zircon grains may have been derived from ancient sources associated with the northern African crustal blocks, such as the Saharan Metacraton and West African craton (STEPHAN et al., 2019a, b). Detrital zircon grains with U-Pb ages of ≈ 1 Ga are characteristic of terrigenous sediment belonging to the Gondwana super-fan system within the East African–Arabian zircon province (MEINHOLD et al., 2021). If we follow the scientific and logical principle often attributed to astronomer Carl Sagan, "absence of evidence is not evidence of absence," then the Mesoproterozoic gap, and especially the ≈ 1 Ga gap, recorded here with only a few sporadic ages, does not confirm nor refute the Saharan Metacraton and/or West African craton as sources. It is possible that zircon of that age span, although we formally met the minimum number of grains required for valid statistical representation in classic provenance studies (95–117; VERMEESCH, 2004), was not representatively sampled – perhaps due to size, habit, or inclusions. However, statistical evaluation of (dis)similarity through the MDS statistical approach (Fig. 4b) points to the Saharan Metacraton as the expected primary source.

5.5. Palaeoproterozoic to Archean ages

Palaeoproterozoic (group 5) to Archean ages (group 6) are almost exclusively related to the zircon cores, including a 3.0 Ga xenocrystic core enveloped by a typical Cadomian zircon rim (≈ 514 Ma; Fig. 4a inset). Palaeoproterozoic to Neoarchean peaks are attributed to basement contributions from the Saharan Metacraton (STEPHAN et al., 2019b; SIEGESMUND et al., 2023). The presence of a Palaeoproterozoic signature therefore supports the existence of Neoarchean and Lower Proterozoic crust (NEUBAUER et al., 2020).

5.6. Statistical links to ancient craton analyses

A simple visual and thus qualitative comparison of the complex age spectrum masked by the abundant younger ages is not straightforward (ŽÁK et al., 2021). Therefore, for a quantitative approach, MDS statistical analysis is often used to identify important relationships among datasets. For MDS, we used compiled datasets of cratonic detrital zircon age spectra from ŽÁK et al. (2021) for four north African source areas: the West African craton, the Trans-Saharan belt, the Saharan Metacraton and the Arabian–Nubian shield. The MDS analysis (Fig. 4b) reveals similarity between age spectra and statistically links the Kutjevo zircon age spectra to the Saharan Metacraton as

the most likely source of zircon grains but also shows possible links to the West African craton and Arabian–Nubian shield and/or their hinterlands. This link is important for understanding the origin of the oldest measured zircon grain, suggesting initial zircon growth in the ancient continental crust of a craton hinterland.

The age distribution reflects transport pathways existing at the time of deposition rather than inheritance from multiple and remote past landscapes (PASTORE et al., 2021). According to MEINHOLD et al. (2013, 2021), the ≈ 1.0 Ga (i.e., Tonian–Stenian) zircons are a key feature of the Gondwana super-fan system, allowing transport from the centre of orogens toward the continental margin of Gondwana. Palaeocurrent markers indicate a northerly direction of sediment transport (i.e. orogen-parallel sediment transport; SQUIRE et al., 2006; YESHANEW et al., 2024) – see Figure 6a. This implies that

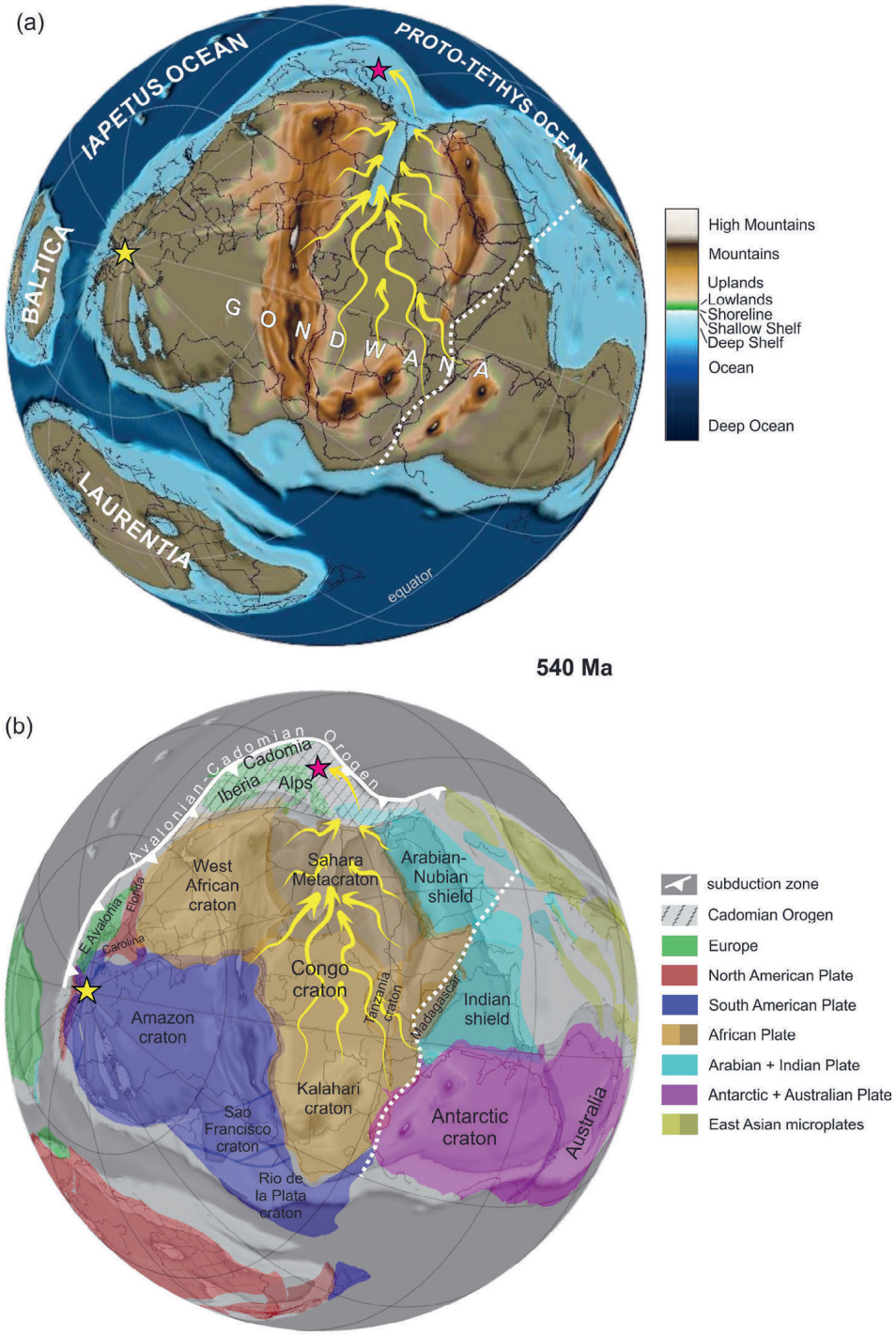

Figure 6. Schematic palaeogeographic reconstruction of Gondwana during the Ediacaran to Cambrian (ca. 540 Ma) using GPlates 2.5.0 (MÜLLER et al., 2018) and palaeomagnetic database of SCOTESE (2016) and MÜLLER et al. (2022), showing the eastern and western north Gondwanan shelves with subduction zone, sediment transport directions and zircon provenance areas (after STEPHAN et al., 2019b). (**a**) Topographic reconstruction and (**b**) reconstruction of the ancient cratons and the palaeogeographic positions of zircon provenance areas (cratonic blocks and interior adjusted with CAWOOD et al., 2021). The position of the south pole is marked with a yellow star. The present-day position of Mt. Papuk in Croatia is marked with a pink star; yellow arrows represent transport direction. White dashed line represents the borderline between Western and Eastern Gondwana.

older material originating from erosion of the central part of the African craton could have been transported and involved in igneous processes when it reached the continental (northern Gondwanan) margin.

At the end of the Proterozoic, the igneous activity at the northern margin of Gondwana in front of the Saharan Metacraton is related to an Andean-type margin in the case of the Caledonian orogeny and/or an Alaskan-type margin in the case of the Cenerian orogeny, where undissolved zircon xenocrysts act as seeds (cores) for newly grown zircon (rim). The old cratons that may be potential candidates as original xenocryst sources are the cratons of Congo, Madagascar and Tanzania (e.g., STEPHAN et al., 2019a, b; MEINHOLD et al., 2021), as well as the Arabian–Nubian shield, which contains zircon grains with ages up to Eoarchaean (3.6–4.0 Ga), the oldest zircon grains yet reported from Arabia (MEINHOLD et al., 2021). These areas may serve as sources for the oldest zircon in central and eastern Europe (Fig. 6).

Among the oldest zircon grains found so far are those in the Bohemian Massif (3.4 Ga; GERDES & FINGER, 2005; cited from LINDNER et al., 2021a) and the Carpathians (3.4 Ga; PUTIŠ et al., 2008). Similar discoveries will undoubtedly be reported in the future, particularly in "unconventional" provenance studies conducted not only on metasediment zircon, but also on (meta)granitoid zircon.

6. CONCLUSION

The zircon age spectrum from a Cambrian peraluminous (meta)granitoid in the eastern part of Mt. Papuk indicates an origin from a complex magmatic felsic source (continental crust) with inherited components. The zircon dates display a pattern beginning with a dominant asymmetric peak composed of age clusters at approximately 498 Ma (Cambrian–Ordovician) and ≈ 535 Ma (Ediacaran–Cambrian), interpreted as a Cenerian thermal event superimposed on the Cadomian granitoid crystallisation age, respectively. Additional smaller age groups and individual data reveal a Pan-African cluster at ≈ 650−800 Ma, along with a gap between ≈ 0.8 and 1.6 Ga, and Palaeoproterozoic clusters inherited from a detrital source (recorded in xenocrystic zircon cores) between 1.6 and 3.0 Ga. The age spectra are characteristic of the Cadomian magmatic event with a superimposed Cenerian signature and further indicate zircon provenance from the western part of northern Gondwana, particularly the Saharan Metacraton, with possible additional contributions from the Arabian–Nubian shield and West African craton, where old zircon grains were transported to the distant northern Gondwana margin from their hinterland. The granitoid crystallisation age of 535.3 ± 0.9 | 7.1 Ma (Early Cambrian) represents the oldest reliably dated rock formation in Croatia, while among the old inherited zircon cores, the oldest mineral measured so far in the Croatian basement has a $^{207}Pb/^{206}Pb$ date of 3061 ± 27 Ma (Mesoarchean). In addition to reporting the "oldest rock" formation and the "oldest mineral", the dataset extracted from the Kutjevo (meta)granitoid is used to reconstruct the source(s) of captured and/or inherited zircon grains, that were eventually gathered and preserved in crystalline rocks of the Mt. Papuk basement.

ACKNOWLEDGEMENT

This study is part of the project "Old orogeny and young magmatism: Cretaceous dyke swarms and their relations to the Variscan basement (Mt. Papuk, Croatia)", which was financially supported by a WTZ Austria-Croatia grant from Austria's Agency for Education and Internationalisation to Daniela GALLHOFER, and by the Croatian Ministry of Science, Education and Youth Austria-Croatia Scientific and Technological Cooperation to Dražen BALEN. The constructive comments of Jiří ŽÁK and Franz NEUBAUER, which helped to improve the manuscript, are greatly appreciated.

REFERENCES

BALEN, D., HORVATH, P., TOMLJENOVIĆ, B., FINGER, F., HUMER, B., PAMIĆ, J. & ÁRKAI, P. (2006): A record of pre-Variscan Barrovian regional metamorphism in the eastern part of the Slavonian Mountains (NE Croatia).– Mineralogy and Petrology, 87/1, 143–162. http://doi.org/10.1007/s00710-006-0120-1

BALEN, D., HORVÁTH, P., FINGER, F. & STARIJAŠ, B. (2013): Phase equilibrium, geothermobarometric and xenotime age dating constraints on the Alpine metamorphism recorded in chloritoid schists from the southern part of the Tisia Mega-Unit (Slavonian Mts., NE Croatia).– International Journal of Earth Sciences, 102, 1091–1109. http://doi.org/10.1007/s00531-012-0850-8

BALEN, D., MASSONNE, H.-J. & PETRINEC, Z. (2015): Collision-related Early Paleozoic evolution of a crustal fragment from the northern Gondwana margin (Slavonian Mountains, Tisia Mega-Unit, Croatia): Reconstruction of the P–T path, timing and paleotectonic implications.– Lithos, 232, 211–228. http://doi.org/10.1016/j.lithos.2015.07.003

BALEN, D., MASSONNE, H.-J. & LIHTER, I. (2018a): Alpine metamorphism of lowgrade schists from the Slavonian Mountains (Croatia): new P-T and geochronological constraints.– International Geology Review, 60/3, 288–304. http://doi.org/10.1080/00206814.2017.1328710

BALEN, D., SCHNEIDER, P., OPITZ, J. & MASSONNE, H.-J. (2018b): Ages and trace element patterns of apatite and zircon in a diorite from the Mt. Papuk metamorphic complex (Pannonian Basin basement in Croatia, CE Europe).– AGU Fall Meeting 2018, V33E-0285. https://ui.adsabs.harvard.edu/abs/2018AGUFM.V33E0285B/abstract

BALEN, D., SCHNEIDER, P., OPITZ, J. & MASSONNE, H.-J. (2018c): REE and trace elements patterns of apatite from a diorite at Mt. Papuk, Croatia.– EGU General Assembly 2018, EGU2018-3843. https://meetingorganizer.copernicus.org/EGU2018/EGU2018-3843.pdf

BALINTONI, I. & BALICA, C. (2013): Avalonian, Ganderian and East Cadomian terranes in South Carpathians, Romania, and Pan-African events recorded in their basement.– Mineralogy and Petrology, 107, 709–725. https://doi.org/10.1007/s00710-012-0206-x

BELOUSOVA, E.A., WALTERS, S., GRIFFIN, W.L., O'REILLY, S.Y. & FISHER, N.I. (2002): Igneous zircon: trace element composition as an indicator of source rock type.– Contributions to Mineralogy and Petrology 143, 602–622. https://doi.org/10.1007/s00410-002-0364-7

BIŠEVAC, V., BALOGH, K., BALEN, D. & TIBLJAŠ, D. (2010): Alpine (Cretaceous) very low- to low-grade metamorphism recorded on the illite-muscovite-rich fraction of metasediments from South Tisia (eastern Mt Papuk, Croatia).– Geologica Carpathica, 61, 469–481. https://doi.org/10.2478/v10096-010-0029-9

BOEHNKE, P., WATSON, E.B., TRAIL, D., HARRISON, T.M. & SCHMITT, A.K. (2013): Zircon saturation re-revisited.– Chemical Geology, 351, 324–334. https://doi.org/10.1016/j.chemgeo.2013.05.028

BORREGO, R.J., POYATOS, D.M., AZOR, A., ACCOTTO, C., JABALOY-SÁNCHEZ, A., LODEIRO, F.G., SABAR, M.S., HAMOUD, A., OULD, A. & LEKOUYRIE, A.O.E. (2026): Persistent Amazonian and West African detrital zircon signature in the northern Mauritanide Belt.– Gondwana Research, 149, 1–16. https://doi.org/10.1016/j.gr.2025.07.026

BRADLEY, D.C., EVANS, D.A.D., O'SULLIVAN, P., TAYLOR, C.D., & EGLINGTON, B.M. (2022): The Assabet barcode: Mesoproterozoic detrital zircons in Neoproterozoic strata from Mauritania, West Africa.– American Journal of Science, 322/8, 939–992. https://doi.org/10.2475/08.2022.01

BURDA, J., KLÖTZLI, U., MAJKA, J., CHEW, D., LI, Q.-L., LIU, Y., GAWĘDA, A. & WIEDENBECK, M. (2021): Tracing proto-Rheic – Qaidam Ocean vestiges into the Western Tatra Mountains and implications for the Palaeozoic palaeogeography of Central Europe.– Gondwana Research, 91, 188–204. https://doi.org/10.1016/j.gr.2020.12.016

CAWOOD, P.A., MARTIN, E.L., MURPHY, J.B. & PISAREVSKY, S.A. (2021): Gondwana's interlinked peripheral orogens.– Earth and Planetary Science Letters, 568, 117057. https://doi.org/10.1016/j.epsl.2021.117057

CHANG, R., NEUBAUER, F., LIU, Y., YUAN, S., GENSER, J., HUANG, Q., GUAN, Q. & YU, S. (2021): Hf isotopic constraints and detrital zircon ages for the Austroalpine basement evolution of Eastern Alps: Review and new data.– Earth-Science Reviews, 221, 103772. https://doi.org/10.1016/j.earscirev.2021.103772

COHEN, K., HARPER, D., GIBBARD, P. & CAR, N. (2025): The ICS international chronostratigraphic chart this decade.– Episodes, 48, 105–115. https://doi.org/10.18814/epiiugs/2025/025001

CROATIAN GEOLOGICAL SURVEY (2009): Geološka karta Republike Hrvatske 1:300.000 [*Geological Map of the Republic of Croatia, 1:300 000* – in Croatian].– Croatian Geological Survey, Department of Geology, Zagreb.

FINGER, F. & RIEGLER, G. (2023): The role of the proto-Alpine Cenerian Orogen in the Avalonian-Cadomian belt.– Austrian Journal of Earth Sciences, 116/71, 109–115. https://doi.org/10.17738/ajes.2023.0005

FINGER, F. & RIEGLER, G. (2025): Revisiting the (pre-Variscan) Galatia/Ligeria – Armorica terrane conception from an Austrian perspective.– Austrian Journal of Earth Sciences, 118, 175–187. https://doi.org/10.17738/ajes.2025.0010

GALLHOFER, D., SKRZYPEK, E., SCHNEIDER, P., BALEN, D. & HAUZENBERGER, C.A. (2026): Contrasting behavior of accessory phases during partial melting of orthogneiss – a case study from Mt. Papuk, Croatia.– Mineralogy and Petrology, 120, 309–332. https://doi.org/10.1007/s00710-026-00975-z

GERDES, A. & FINGER, F. (2005): Über die ältesten Zirkone Österreichs und neue Möglichkeiten in der Grundgebirgsforschung durch Einsatz moderner Laser-Ablation-ICP-MS Zirkonanalytik [in German].– Mitteilungen der Österreichischen Mineralogischen Gesellschaft, 151, 44.

HAAS, I., EICHINGER, S., HALLER, D., FRITZ, H., NIEVOLL, J., MANDL, M., HIPPLER, D. & HAUZENBERGER, C. (2020): Gondwana fragments in the Eastern Alps: A travel story from U/Pb zircon data.– Gondwana Research, 77, 204–222. https://doi.org/10.1016/j.gr.2019.07.015

HORSTWOOD, M.S.A., KOŠLER, J., GEHRELS, G., JACKSON, S.E., MCLEAN, N.M., PATON, C., PEARSON, N.J., SIRCOMBE, K., SYLVESTER, P., VERMEESCH, P., BOWRING, J.F., CONDON, D.J. & SCHOENE, B. (2016): Community-Derived Standards for LA-ICP-MS U-(Th-)Pb Geochronology – Uncertainty Propagation, Age Interpretation and Data Reporting.– Geostandards and Geoanalytical Research, 40, 311–332. https://doi.org/10.1111/j.1751-908X.2016.00379.x

HORVAT, M., KLÖTZLI, U., JAMIČIĆ, D., BUDA, G., KLÖTZLI., E. & HAUZENBERGER, CH. (2018): Geochronology of granitoids from Psunj and Papuk Mts., Croatia.– Geochronometria, 45/1, 198–210. https://doi.org/10.1515/geochr-2015-0099

HORVÁTH, P., BALEN, B., FINGER, F., TOMLJENOVIĆ, B. & KRENN, E. (2010): Contrasting P-T-t paths from the basement of the Tisia Unit (Slavonian Mts., NE Croatia): application of quantitative phase diagrams and monazite age dating.– Lithos, 117, 269–282. https://doi.org/10.1016/j.lithos.2010.03.004

JACKSON, S.E., PEARSON, N.J., GRIFFIN, W.L. & BELOUSOVA, E.A. (2004): The application of laser ablation-inductively coupled plasma-mass spectrometry to in situ U–Pb zircon geochronology.– Chemical Geology, 211, 47–69. https://doi.org/10.1016/j.chemgeo.2004.06.017

JAMIČIĆ, D. (1983): Strukturni sklop metamorfnih stijena Krndije i južnih padina Papuka [*Structural fabric of the metamorphosed rocks of Mt. Krndija and the eastern part of Mt. Papuk* – in Croatian, with an English summary].– Geološki vjesnik, 36, 51–72.

JAMIČIĆ, D. (1988): Strukturni sklop slavonskih planina [*Structural fabric of the Slavonian Mts. (northern Papuk, Psunj, Krndija)* – in Croatian, with an English summary].– PhD Thesis, Faculty of Science, University of Zagreb, 152 p.

JAMIČIĆ, D. (1989): Osnovna geološka karta SFRJ 1:100 000, list Daruvar 1:100 000 L 33-95 [*Basic Geological Map of SFRY 1:100 000, Daruvar sheet L 33-95* – in Croatian].– Institut za geološka istraživanja, Zagreb, Savezni geološki zavod, Beograd.

JAMIČIĆ, D. & BRKIĆ, M. (1987): Osnovna geološka karta SFRJ 1:100.000, list Orahovica L 33-96 [*Basic Geological Map of SFRY 1:100,000, Orahovica sheet L 33-96* – in Croatian].– Institut za geološka istraživanja, Zagreb, Savezni geološki zavod, Beograd.

JAMIČIĆ, D., BRKIĆ, M., CRNKO, J. & VRAGOVIĆ, M. (1987): Osnovna geološka karta SFRJ 1:100 000. Tumač za list Orahovica L 33-96 *[Basic Geological Map of SFRY 1:100 000. Explanatory notes for the Orahovica sheet L 33-96* – in Croatian].– Institut za geološka istraživanja, Zagreb, Savezni geološki zavod, Beograd, 72 p.

JAMIČIĆ, D., VRAGOVIĆ, M. & MATIČEC, D. (1989) Osnovna geološka karta SFRJ 1:100 000. Tumač za list Daruvar L 33-95[*Basic Geological Map of SFRY 1:100 000. Explanatory notes for the Daruvar sheet L 33-95* – in Croatian].– Institut za geološka istraživanja, Zagreb, Savezni geološki zavod, Beograd, 53 p.

JOCHUM, K.P., WEIS, U., STOLL, B., KUZMIN, D., YANG, Q., RACZEK, I., JACOB, D.E., STRACKE, A., BIRBAUM, K., FRICK, D.A., GÜNTHER, D. & ENZWEILER, J. (2011): Determination of reference values for NIST SRM 610–617 glasses following ISO guidelines.– Geostandards and Geoanalytical Research, 35, 397–429. https://doi.org/10.1111/j.1751-908X.2011.00120.x

KLUG, L., FROITZHEIM, N. & TOMASCHEK, F. (2025): Zircon ages and differentiation trend of Ordovician granitoids from the southeastern Ötztal Nappe (Texelgruppe, South Tyrol, Italy): ridge subduction at the margin of Gondwana?– Austrian Journal of Earth Sciences, 118, 95–114. https://doi.org/10.17738/ajes.2025.0005

KOHÚT, M., LINNEMANN, U., HOFMANN, M., GÄRTNER, A. & ZIEGER, J. (2022): Provenance and detrital zircon study of the Tatric Unit basement (Western Carpathians, Slovakia).– International Journal of Earth Sciences, 111, 2149–2168. https://doi.org/10.1007/s00531-022-02224-y

LINDNER, M., DÖRR, W., HAUZENBERGER, C.A., REITHER, D. & FINGER, F. (2021a): In search of the oldest rock of Austria: The Hauergraben Gneiss, a 1.40 Ga old mafic quartz-monzonitic inlayer in the Dobra Gneiss (Drosendorf Unit, Bohemian Massif) as a new candidate.– Austrian Journal of Earth Sciences, 114, 29–45. https://doi.org/10.17738/ajes.2021.0002

LINDNER, M., DÖRR, W., REITHER, D. & FINGER, F. (2021b): The Dobra Gneiss and the Drosendorf Unit in the southeastern Bohemian Massif, Austria: West Amazonian crust in the heart of Europe.– Geological Society London Special Publications, 503/1, 185–207. https://doi.org/10.1144/SP503-2019-232

MEINHOLD, G., BASSIS, A., HINDERER, M., LEWIN, A. & BERNDT, J. (2021): Detrital zircon provenance of north Gondwana Palaeozoic sandstones from Saudi Arabia.– Geological Magazine, 158, 442–458. https://doi.org/10.1017/S0016756820000576

MEINHOLD, G., MORTON, A.C. & AVIGAD, D. (2013): New insights into peri-Gondwana paleogeography and the Gondwana super-fan system from detrital zircon U–Pb ages.– Gondwana Research, 23, 661–665. https://doi.org/10.1016/j.gr.2021.05.003

MÜLLER, R.D., CANNON, J., QIN, X., WATSON, R.J., GURNIS, M., WILLIAMS, S., PFAFFELMOSER, T., SETON, M., RUSSELL, S.H.J. & ZAHIROVIC, S. (2018): GPlates: building a virtual Earth through deep time.– Geochemistry, Geophysics, Geosystems 19, 2243–2261. https://doi.org/10.1029/2018GC007584

MÜLLER, R.D., CANNON, J., TETLEY, M., WILLIAMS, S.E., CAO, X., FLAMENT, N., BODUR, Ö.F., ZAHIROVIC, S. & MERDITH, A. (2022): A tectonic-rules based mantle reference frame since 1 billion years ago–implications for supercontinent cycles and plate-mantle system evolution.– Solid Earth, 13, 1127–1159. https://doi.org/10.5194/se-13-1127-2022

NANCE, R.D., MURPHY, J.B., STRACHAN, R.A., KEPPIE, J.D., GUTIÉRREZ-ALONSO, G., FERNÁNDEZ-SUÁREZ, J., QUESADA, C., LINNEMANN, U., D'LEMOS, R. & PISAREVSKY, S.A. (2008): Neoproterozoic – early Palaeozoic tectonostratigraphy and palaeogeography of the peri-Gondwanan terranes: Amazonian v. West African connections.– Geological Society London Special Publications, 297, 345–383. https://doi.org/10.1144/SP297.17

NANCE, R.D., GUTIERREZ-ALONSO, G., KEPPIE, J.D., LINNEMANN, U., MURPHY, J.B., QUESADA, C., STRACHAN, R.A. & WOODCOCK, N.H. (2010): Evolution of the Rheic Ocean.– Gondwana Research, 17, 194–222. https://doi.org/10.1016/j.gr.2009.08.001

NASDALA, L., HOFMEISTER, W., NORBERG, N., MARTINSON, J.M., CORFU, F., DÖRR, W., KAMO, S.L., KENNEDY, A.K., KRONZ, A., REINERS, P.W., FREI, D., KOŠLER, J., WAN, Y., GÖTZE, J., HÄGER, T., KRÖNER, A. & VALLEY, J.W. (2008): Zircon M257 – a Homogeneous Natural Reference Material for the Ion Microprobe U-Pb Analysis of Zircon.– Geostandards and Geoanalytical Research, 32, 247–265. https://doi.org/10.1111/j.1751-908X.2008.00914.x

NEUBAUER, F., FRISCH, W. & HANSEN, B.T. (2002): Early Palaeozoic tectonothermal events in basement complexes of the eastern Greywacke Zone (Eastern Alps): evidence from U-Pb zircon data.– International Journal of Earth Science, 91, 775–786. https://doi.org/10.1007/s00531-001-0254-7

NEUBAUER, F., LIU, Y., CHANG, R., YUAN, S., YU, S., GENSER, J., LIU, B. & GUAN, Q. (2020): The Wechsel Gneiss Complex of Eastern Alps: an Ediacaran to Cambrian continental arc and its Early Proterozoic hinterland.– Swiss Journal of Geosciences, 113, 21. https://doi.org/10.1186/s00015-020-00373-3

NEUBAUER, F., LIU, Y., DONG, Y., CHANG, R., GENSER, J. & YUAN, S. (2022): Pre-Alpine tectonic evolution of the Eastern Alps: from Prototethys to Paleotethys.– Earth-Science Reviews, 226, 103923. https://doi.org/10.1016/j.earscirev.2022.103923

ORIOLO, S., SCHULZ, B., GEUNA, S., GONZÁLEZ, P.D., OTAMENDI, J.E., SLÁMA, J., DRUGUET, E. & SIEGESMUND, S. (2021): Early Paleozoic accretionary orogens along the Western Gondwana margin.– Geoscience Frontiers, 12/1, 109–130. https://doi.org/10.1016/j.gsf.2020.07.001

PAMIĆ, J. & LANPHERE, M. (1991): Hercynian granites and metamorphic rocks from the Papuk, Psunj, Krndija and the surrounding basement of the Pannonian Basin (Northern Croatia, Yugoslavia).– Geologija, 34, 81–253.

PAMIĆ, J., LANPHERE, M. & MCKEE, E. (1988): Radiometric ages of metamorphic and associated igneous rocks of the Slavonian Mountains in the southern part of the Pannonian basin.– Acta Geologica, 18, 13–39.

PAMIĆ, J., BALEN, D. & TIBLJAŠ, D. (2002): Petrology and geochemistry of orthoamphibolites from the Variscan metamorphic sequences of the South Tisia in Croatia – an overview with geodynamic implications.– International Journal of Earth Sciences, 91, 787–798. https://doi.org/10.1007/s00531-002-0258-y

PASTORE, G., BAIRD, T., VERMEESCH, P., BRISTOW, C., RESENTINI, A. & GARZANTI, E. (2021): Provenance and recycling of Sahara Desert sand.– Earth-Science Reviews, 216, 103606. https://doi.org/10.1016/j.earscirev.2021.103606

PASTORE, G., GARZANTI, E., VERMEESCH, P., BAYON, G., RESENTINI, A., BRAQUET, N. & OVERARE, B. (2023): The zircon story of the Niger River: Time-structure maps of the West African Craton and discontinuous propagation of provenance signals across a disconnected sediment-routing system.– Journal of Geophysical Research: Earth Surface, 128, e2023JF007342. https://doi.org/10.1029/2023JF007342

PATON, C., WOODHEAD, J.D., HELLSTROM, J.C., HERGT, J.M., GREIG, A. & MAAS, R. (2010): Improved laser ablation U-Pb zircon geochronology through robust downhole fractionation correction.– Geochemistry, Geophysics, Geosystems, 11, Q0AA06. https://doi.org/10.1029/2009GC002618

PATON, C., HELLSTROM, J.C., PAUL, B., WOODHEAD, J.D. & HERGT, J.M. (2011): Iolite: Freeware for the visualisation and processing of mass spectrometric data.– Journal of Analytical Atomic Spectrometry, 26, 2508–2518. https://doi.org/10.1039/C1JA10172B

PETRÍK, I., JANÁK, M., FINGER, F., KURYLO, S., KONEČNÝ, P. & VACULOVIČ, T. (2024): Ordovician (Cenerian) metamorphism in the Western Carpathians: Evidence from EMP monazite dating of polymetamorphosed granitoids in the Veporic unit, Slovakia.– Lithos, 476, 107600. https://doi.org/10.1016/j.lithos.2024.107600

PUPIN, J.P. (1980): Zircon and granite petrology.– Contributions to Mineralogy and Petrology,73, 207–220. https://doi.org/10.1007/BF00381441

PUTIŠ, M., SERGEEV, S., ONDREJKA, M., LARIONOV, A., SIMAN, P., SPIŠIAK, J., UHER, P. & PADERIN, I. (2008): Cambrian-Ordovician metaigneous rocks associated with Cadomian fragments in the West-Carpathian basement dated by SHRIMP on zircons: a record from the Gondwana active margin setting.– Geologica Carpathica, 59, 3–18.

SCHMID, S.M., BERNOULLI, D., FÜGENSCHUH, B., MATENCO, L., SCHEFER, S., SCHUSTER, R., TISCHLER, M. & USTASZEWSKI, K. (2008): The Alpine-Carpathian-Dinaridic orogenic system: correlation and evolution of tectonic units.– Swiss Journal of Geosciences, 101, 139–183. https://doi.org/10.1007/s00015-008-1247-3

SCHNEIDER, P., BALEN, D., OPITZ, J. & MASSONNE, H.-J. (2022): Dating and geochemistry of zircon and apatite from rhyolite at the UNESCO geosite Rupnica (Mt. Papuk, northern Croatia) and the relationship to the Sava Zone.– Geologia Croatica, 75, 249–267. https://doi.org/10.4154/gc.2022.19

SCHNEIDER, P., GALLHOFER, D., SKRZYPEK, E., HAUZENBERGER, C.A. & BALEN, D. (2025): Age and origin of a brief Late Cretaceous magmatic pulse based on geochemical data from accessory zircon: A case study from Mt. Papuk, Croatia.– Geologica Carpathica, 76/4, 277–299. https://doi.org/10.31577/GeolCarp.2025.13

SIEGESMUND, S., ORIOLO, S., HEINRICHS, T., BASEI, M.A.S., NOLTE, N., HÜTTENRAUCH, F. & SCHULZ, B. (2018): Provenance of Austroalpine basement metasediments: tightening up Early Palaeozoic connections between peri-Gondwanan domains of central Europe and Northern Africa.– International Journal of Earth Sciences, 107, 2293–2315. https://doi.org/10.1007/s00531-018-1599-5

SIEGESMUND, S., ORIOLO, S., SCHULZ, B., HEINRICHS, T., BASEI, M.A.S. & LAMMERER, B. (2021): The birth of the Alps: Ediacaran to Paleozoic accretionary processes and crustal growth along the northern Gondwana margin.– International Journal of Earth Sciences, 110/4, 1321–1348. https://doi.org/10.1007/s00531-021-02019-7

SIEGESMUND, S., ORIOLO, S., BROGE, A., HUECK, M., LAMMERER, B., BASEI, M.A.S. & SCHULZ, B. (2023): Cadomian to Cenerian accretionary orogenic processes in the Alpine basement: the detrital zircon archive.– International Journal of Earth Sciences, 112/4, 1157–1174. https://doi.org/10.1007/s00531-023-02305-6

SKRZYPEK, E., GALLHOFER, D., BALEN, D., SCHNEIDER, P. & HAUZENBERGER, C.A. (2025): "Dry" and "wet" alteration of magmatic monazite in Variscan crystalline rocks from Mt. Papuk (Croatia).– Geologica Carpathica, 76/3, 189−208. https://doi.org/10.31577/GeolCarp.2025.10

SLÁMA, J., KOŠLER, J., CONDON, D.J., CROWLEY, J.L., GERDES, A., HANCHAR, J.M., HORSTWOOD, M.S., MORRIS, G.A., NASDALA, L., NORBERG, N., SCHALTEGGER, U., SCHOENE, B., TUBRETT, M.N. & WHITEHOUSE, M.J. (2008): Plešovice zircon – A new natural reference material for U–Pb and Hf isotopic microanalysis.– Chemical Geology, 249, 1–35. https://doi.org/10.1016/j.chemgeo.2007.11.005

SLOVENEC, D., BELAK, M., MIŠUR, I., ŠEGVIĆ, B. & SCHUSTER, R. (2020): The early Paleozoic cumulate gabbroic rocks from the southwest part of the Tisza Mega-Unit (Mt. Papuk, NE Croatia): evidence of a Gondwana suture zone.– International Journal of Earth Sciences, 109, 2209–2233. https://doi.org/10.1007/s00531-020-01896-8

SPAHIĆ, D., MILOVANOVIĆ, D., KOSTIĆ, B., KUREŠEVIĆ, L. & TANČIĆ, P. (2025): Reconstruction of the enigmatic pre-Variscan paleogeographic configuration of the western peri-Moesian realm (Carpathian-Balkans, eastern Serbia): An insight into Devonian small-scale continental and paleo-oceanic units.– Earth Science Reviews, 270, 105227. https://doi.org/10.1016/j.earscirev.2025.105227

SQUIRE, R.J., CAMPBELL, I.H., ALLEN, C.M. & WILSON, C.J.L. (2006): Did the Transgondwanan Supermountain trigger the explosive radiation of animals on earth?– Earth and Planetary Science Letters, 250/1–2, 116–133. https://doi.org/10.1016/j. epsl.2006.07.032

STARIJAŠ MAYER, B., ZEH, A., KRENN, E., GERDES, A. & FINGER, F. (2023): Tracing the cryptic Sardic (Ordovician) metamorphism across Alpine Europe: the Krndija region in the Slavonian Mountains, Croatia.– International Journal of Earth Sciences, 112, 829–853. https://doi.org/10.1007/s00531-022-02282-2

STEPHAN, T., KRONER, U. & ROMER, R.L. (2019a): The pre-orogenic detrital zircon record of the Peri-Gondwanan crust.– Geological Magazine, 156/2, 281–307. https://doi.org/10.1017/S0016756818000031

STEPHAN, T., KRONER, U., ROMER, R.L. & RÖSEL, D. (2019b): From a bipartite Gondwana shelf to an arcuate Variscan belt: the early Paleozoic evolution of northern Peri-Gondwana.– Earth-Science Reviews, 192, 491–512. https://doi.org/10.1016/j.earscirev.2019.03.012

STOICA, A.M., DUCEA, M.N., ROBAN, R.D. & JIANU, D. (2016): Origin and evolution of the South Carpathians basement (Romania): a zircon and monazite geochronologic study of its Alpine sedimentary cover.– International Geology Review, 58/4, 510–524. https://doi.org/10.1080/00206814.2015.1092097

SZEMERÉDI, M., VARGA, A., DUNKL, I., LUKÁCS, R., RAUCSIK, B. & PÁL-MOLNÁR, E. (2025): Constraints on Ordovician and Carboniferous magmatism in the Carpathian–Pannonian region: New petrological and geochronological insights from the Tisza–Dacia and ALCAPA Mega-units (Hungary and Romania).– Geologica Carpathica, 76/4, 259–276. https://doi.org/10.31577/GeolCarp.2025.17

VERMEESCH, P. (2004): How many grains are needed for a provenance study?– Earth and Planetary Science Letters, 224, 441–451. https://doi.org/10.1016/j.epsl.2004.05.037

VERMEESCH, P. (2012): On the visualization of detrital age distributions.– Chemical Geology, 312–313, 190–194. https://doi.org/10.1016/j.chemgeo.2012.04.021

VERMEESCH, P. (2018): IsoplotR: A free and open toolbox for geochronology.– Geoscience Frontiers, 9, 1479–1493. https://doi.org/10.1016/j.gsf.2018.04.001

VESELÁ, P., ORIOLO, S., BASEI, M.A.S., LAMMERER, B. & SIEGESMUND, S. (2022): The detrital zircon record of Variscan to post-Variscan tectonosedimentary and magmatic processes in the Tauern Window (Eastern Alps).– International Journal of Earth Science, 111, 1273–1287. https://doi.org/10.1007/s00531-022-02179-0

WATSON, E.B., WARK, D.A. & THOMAS, J.B. (2006): Crystallization thermometers for zircon and rutile.– Contributions to Mineralogy and Petrology, 151, 413–433. https://doi.org/10.1007/s00410-006-0068-5

WIEDENBECK, M., ALLÉ, P., CORFU, F., GRIFFIN, W.L., MEIER, M., OBERLI, F., VON QUADT, A., RODDICK, J.C. & SPIEGEL, W. (1995): Three natural zircon standards for U-Th-Pb, Lu-Hf, trace element and REE analyses.– Geostandards Newsletter, 19, 1–23. https://doi.org/10.1111/j.1751-908X.1995.tb00147.x

YESHANEW, F.G., WHITEHOUSE, M.J., PEASE, V., BADENSZKI, E. & DALY, J.S. (2024): Continental-scale sediment mixing and dispersal across northern Gondwana: detrital zircon U-Pb-O-Hf isotopic evidence from the Cambro-Ordovician sandstones overlying the Arabian Shield.– International Geology Review, 67/3, 285–305. https://doi.org/10.1080/00206814.2024.2392142

ŽÁK, J., SVOJTKA, M., GERDJIKOV, I., KOUNOV, A. & VANGELOV, D.A. (2021): The Balkan terranes: a missing link between the eastern and western segments of the Avalonian–Cadomian orogenic belt?– International Geology Review, 64/17, 2389-2415. https://doi.org/10.1080/00206814.2020.1861486

ZEH, A., HINDERER, M., DIEHL, C. & GERDES, A. (2025): U–Pb–Hf isotope and shape systematics of detrital zircon populations from the Badenweiler–Lenzkirch Zone, Black Forest (Germany): new constraints on sediment deposition, provenance and Variscan evolution.– International Journal of Earth Sciences, 114, 1051–1071. https://doi.org/10.1007/s00531-025-02532-z

ZURBRIGGEN, R. (2015): Ordovician orogeny in the Alps: a reappraisal.– International Journal of Earth Sciences, 104/2, 335–350. https://doi.org/10.1007/s00531-014-1090-x

ZURBRIGGEN, R. (2017): The Cenerian orogeny (early Paleozoic) from the perspective of the Alpine region.– International Journal of Earth Sciences, 106/2, 517–529. https://doi.org/10.1007/s00531-016-1438-5

ZURBRIGGEN, R. (2020): Banded amphibolites in the Alps: a new interpretation in relation to early Paleozoic peraluminous magmatism.– Swiss Journal of Geosciences, 113/1, 1–24. https://doi.org/10.1186/s00015-020-00362-6

Web source:

SCOTESE, C.R. (2016): PALEOMAP PaleoAtlas for GPlates and the PaleoData Plotter Program, PALEOMAP project. Available at: https://www.earthbyte.org/paleomap-paleoatlas-for-gplates/. Accessed on: February 27th, 2026.

Electronic supplementary material is available online at
http://www.geologia-croatica.hr